

Chapter 5

The Physical hydroclimate system of the Amazon



Vista aérea da Terra Indígena Yanomami (Foto: Bruno Kelly/Amazônia Real)



Science Panel for the Amazon



About the Science Panel for the Amazon (SPA)

The Science Panel for the Amazon is an unprecedented initiative convened under the auspices of the United Nations Sustainable Development Solutions Network (SDSN). The SPA is composed of over 200 preeminent scientists and researchers from the eight Amazonian countries, French Guiana, and global partners. These experts came together to debate, analyze, and assemble the accumulated knowledge of the scientific community, Indigenous peoples, and other stakeholders that live and work in the Amazon.

The Panel is inspired by the Leticia Pact for the Amazon. This is a first-of-its-kind Report which provides a comprehensive, objective, open, transparent, systematic, and rigorous scientific assessment of the state of the Amazon's ecosystems, current trends, and their implications for the long-term well-being of the region, as well as opportunities and policy relevant options for conservation and sustainable development.

Amazon Assessment Report 2021, Copyright @ 2021, Science Panel for the Amazon.

This report is published under a Creative Commons Attribution-NonCommercial-ShareAlike 4.0 International (CC BY-NC-SA 4.0) License. ISBN: 9781734808001

Suggested Citation

Costa MH, Borma LS, Espinoza JC, Macedo M, Marengo JA, Marra DM, Ometto JP, Gatti LV. 2021. Chapter 5: The physical hydroclimate system of the Amazon. In: Nobre C, Encalada A, Anderson E, Roca Alcazar FH, Bustamante M, Mena C, Peña-Claros M, Poveda G, Rodriguez JP, Saleska S, Trumbore S, Val AL, Villa Nova L, Abramovay R, Alencar A, Rodríguez Alzza C, Armenteras D, Artaxo P, Athayde S, Barretto Filho HT, Barlow J, Berenguer E, Bortolotto F, Costa FA, Costa MH, Cuvi N, Fearnside PM, Ferreira J, Flores BM, Frieler S, Gatti LV, Guayasamin JM, Hecht S, Hirota M, Hoorn C, Josse C, Lapola DM, Larrea C, Larrea-Alcazar DM, Lehm Ardaya Z, Malhi Y, Marengo JA, Melack J, Moraes R M, Moutinho P, Murmis MR, Neves EG, Paez B, Painter L, Ramos A, Rosero-Peña MC, Schmink M, Sist P, ter Steege H, Val P, van der Voort H, Varese M, Zapata-Ríos G (Eds). Amazon Assessment Report 2021. United Nations Sustainable Development Solutions Network, New York, USA. Available from <https://www.theamazonwewant.org/spa-reports/>. DOI: 10.55161/HTSD9250

INDEX

GRAPHICAL ABSTRACT	5.2
KEY MESSAGES.....	5.3
ABSTRACT	5.3
5.1 INTRODUCTION.....	5.4
5.2 MAIN FEATURES OF THE AMAZON CLIMATE.....	5.5
5.2.1 SPATIAL DISTRIBUTION OF CLIMATE VARIABLES	5.5
5.2.1.1 <i>Air temperature</i>	5.5
5.2.1.2 <i>Atmospheric circulation</i>	5.6
5.2.1.3 <i>Rainfall</i>	5.7
5.2.2 THE ROLE OF ENSO AND OTHER LARGE-SCALE MECHANISMS.....	5.7
5.2.2.1 <i>ENSO</i>	5.7
5.2.2.2 <i>PDO, AMO, MJO</i>	5.8
5.2.3. EXTREME DROUGHT AND FLOOD EVENTS	5.8
5.2.4 ANDEAN-AMAZON HYDROMETEOROLOGY AND VARIABILITY	5.9
5.2.4.1 <i>Seasonal patterns</i>	5.9
5.2.4.2 <i>Interannual variability and extremes</i>	5.11
5.3 THE AMAZON CONVECTION AND MESOSCALE CIRCULATIONS	5.12
5.3.1 NATURE OF THE AMAZON CONVECTION	5.12
5.3.2 SOLAR FORCING	5.13
5.3.3 FOREST BREEZE AND RIVER BREEZE CIRCULATIONS.....	5.14
5.3.4 SEA BREEZE AND COASTAL CIRCULATIONS	5.15
5.3.5 OROGRAPHIC-INDUCED CIRCULATIONS AND SPATIAL RAINFALL DISTRIBUTION IN THE ANDEAN-AMAZON REGION	5.15
5.3.6 THE ROLE OF EXTREME WEATHER EVENTS ON ECOSYSTEM DYNAMICS.....	5.16
5.3.6.1 <i>Severe storms, blowdowns, and impacts on forest ecosystem dynamics</i>	5.17
5.3.6.2 <i>Lightning, natural fires, and impacts on vegetation structure and biome distribution</i>	5.18
5.4 EVAPOTRANSPIRATION.....	5.19
5.5 MAIN CHARACTERISTICS OF THE SURFACE HYDROLOGICAL SYSTEMS IN THE AMAZON.....	5.21
5.5.1 SEASONALITY OF DISCHARGE.....	5.21
5.5.2 SEASONALITY OF FLOODPLAIN DYNAMICS	5.23
5.6 THE ROLE OF RIVERS IN BIOGEOCHEMICAL CYCLES.....	5.23
5.7 CONCLUSIONS	5.24
5.8 RECOMMENDATIONS.....	5.24
5.9 REFERENCES.....	5.25

Graphical Abstract

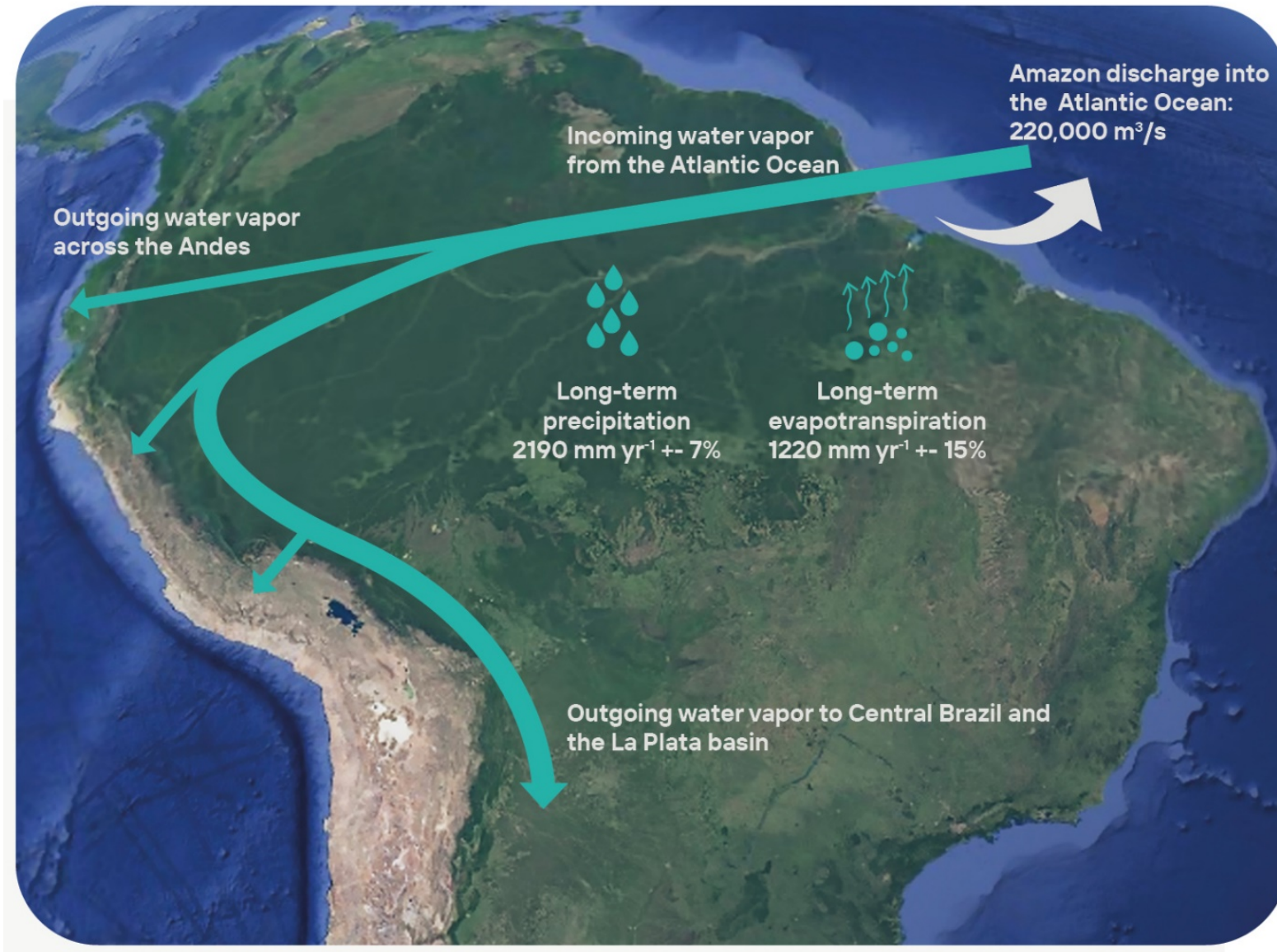


Figure 5.. Graphical Abstract

The physical hydroclimate system of the Amazon

Marcos H. Costa^a, Laura S. Borma^b, Jhan C. Espinoza^c, Marcia Macedo^d, José A. Marengo^e, Daniel M. Marra^f, Jean P. Ometto^b, Luciana V. Gatti^b

Key Messages

- Given its tropical location enclosed by the Andes, its huge spatial extent (7.3 million km², including the Tocantins), and forest cover, the Amazon River Basin is one of the most critical elements of the Earth's climate system. It is the largest and most intense land-based convective center, exerting a strong influence on atmospheric dynamics and circulation patterns both within and outside the tropics. It produces rainfall that results in the largest river discharges on Earth at 220,000 m³/s, corresponding to 16-22% of the total world river discharge.
- The Amazon Basin is mainly characterized by lowlands with a warm and rainy climate. The upper part of the basin includes the eastern slope of the Andes, characterized by a wide variety of mountain climates (cloud forest, Páramos, Yungas, Punas, etc.).
- The El Niño-Southern Oscillation (ENSO) is the main cause of interannual variability in rainfall. ENSO is typically (but not exclusively) accompanied by droughts in the Amazon region, with recent severe droughts producing low river water levels, a high risk of forest fires, and impacts on natural river ecosystems. In addition to ENSO, Atlantic and Pacific SST variability influence the climate of the Amazon at interannual and interdecadal time-scales, including extreme events.
- In the last 15 years, the Amazon has witnessed several climate extremes: droughts in 2005, 2010, and 2015–16 and floods in 2009, 2013, 2014, and 2017, and 2021. Some of these have been classified as "once-in-a-century" events. Historical records show previous droughts in 1926, 1964, 1980, 1983, and 1998 and floods in 1953, 1988, and 1989.

Abstract

The physical hydroclimate system of the Amazon operates on several spatial and temporal scales. Large-scale processes, including solar forcing, control the main seasonal patterns of atmospheric circulation, rainfall, river discharge, and flooding. For example, persistent patterns of sea surface temperature, such as those associated with the El Niño/Southern Oscillation, are associated with the main modes of interannual and interdecadal climate variability. Mesoscale processes such as those related to topography or land-atmosphere interactions cause other localized circulations. While the ultimate source of water in the basin is evaporation from the oceans, this water is recycled through evaporation and reprecipitation before being exported back to the ocean through the flow of the Amazon River or exported in the form of water vapor from the basin. The abundant rainfall in the Amazon Basin (averaging 2,190 mm per year) is thus a consequence of intense radiative heating, low-level convergence of oceanic water vapor, and permanent re-injection of water vapor into the atmosphere by the rainforest itself, aided by the mechanical

^a Dept. of Agricultural Engineering, Federal University of Viçosa (UFV), Viçosa, MG, Brazil

^b National Institute for Space Research (INPE), S. J. Campos, SP, Brazil

^c Université Grenoble Alpes, IRD, CNRS, G-INP, IGE (UMR 5001), Grenoble, France

^d Woodwell Climate Research Center, Falmouth, MA, United States

^e Centro Nacional de Monitoramento e Alertas de Desastres Naturais (CEMADEN), Estrada Doutor Altino Bondensan, 500, Distrito de Eugênio de Melo, São José dos Campos SP, Brazil

^f Max-Planck Institute for Biogeochemistry (MPI-BGC), Jena, Germany

uplifting of air by the Andes. Land surface processes partition precipitation into evapotranspiration (~1,220 mm per year), surface runoff, and deep drainage to the groundwater. The Amazon River system drains the surface and groundwater components of this abundant rainfall, forming the world's largest watershed and feeding the world's largest river, with a mean discharge of 220,000 m³/s. The Amazon has a discharge five times larger than the Congo, the world's second-largest river. The flow is highly seasonal, and imbalances between the addition of water to rivers by rainfall and the rate of water export downstream cause seasonal flooding over a large floodplain area, with beneficial ecological and biogeochemical implications. Extreme flood and drought events are associated with intense interannual rainfall variability, which, in turn, influence forest fires and biogeochemical cycles.

Keywords: Amazon water balance, extreme events

5.1 Introduction

The Amazon is one of the three permanent centers of convection in the intertropical zone (along with Central Africa and Southeast Asia) – i.e., one of the main centers of ascending air that transports energy from land to the atmosphere. It is also the most powerful of these three land-based convective centers, exerting strong influences on atmospheric circulation both within and outside the tropics. As one of the main drivers of the Hadley-Walker circulations, the Amazon is a critical energy source to the atmosphere, removing latent heat from the surface by evaporation and transpiration of water (a process termed evapotranspiration), and releasing that heat to the atmosphere when water condenses and forms clouds or precipitation. The strength of the Amazon convective center is mainly due to its geographical characteristics, including its large size, position spanning the equator, and the presence of the Andes mountains located downwind in the basin. As explained throughout this chapter, the rainforest also contributes to strengthening this convective center. The low albedo of the rainforest increases the absorbed net radiation, and the constant flux of water vapor to the atmosphere from the rainforest via evapotranspiration adds energy to the mean convection fields. At the same time, it smooths seasonal and interannual variability of convection and rainfall in the region.

The region's abundant convection and rainfall, along with the basin's large size, produce the world's largest river, flanked by a complex network

of channels and floodplains that transport sediments, carbon, and other nutrients. Intense seasonality and interannual variability of the water cycle are also dominant factors for local riverine communities who may have their towns either flooded or completely isolated depending on the status of this river system – dictated by the modes of interannual climate variability of rainfall (Marengo and Espinoza, 2016).

Table 1 presents a synthesis of several estimates of the Amazon River Basin's long-term water balance. Long-term estimates of precipitation (P) show little variability across studies, with a median value of ~2190 mm/yr±7%.

The long-term mean runoff (R) is estimated at 1100 mm/yr±15%, which yields a median runoff coefficient ($C=R/P$) of 0.51 ± 0.08 .

Estimates of evapotranspiration (ET) have much higher uncertainties by comparison, with median values of ~1250 mm/yr±50%. This imbalance is likely because most high estimates of ET (>1500 mm/yr) are derived from reanalysis data, which (by design) do not conserve mass over the long-term. If these high values are excluded, the median value of ET is closer to 1220 mm/yr±15%, with a median evaporative fraction ($EF = ET/P$) of 0.54 ± 0.07 . Over the long term the total rainfall must be partitioned either into runoff or evaporation. Table 1 shows estimates of this balance made in the literature – with many estimates splitting precipitation evenly between ET and runoff.

Table 5.1. Long-term water balance of the Amazon river basin according to several studies. Studies marked by an asterisk (*) include the Tocantins river basin. Precipitation (P), evapotranspiration (ET), runoff (R), and the imbalance (P – ET – R) are expressed in mm/yr. The runoff coefficient (C = R/P) and evaporative fraction (EF=ET/P) are dimensionless variables.

Studies	Period	P	R	ET	C	EF	Imbalance
					(R/P)	(ET/P)	P-E-R
Costa and Foley (1999)*	1976-1996	2160	1106	1679	0.51	0.78	-625
Zeng (1999)	1985-1993	2044	1095	1879	0.54	0.92	-930
Salazar (2004)	1961-1990	2189	940	1248	0.43	0.57	1
Marengo (2004)*	1970-1999	2117	1059	1570	0.5	0.74	-512
Getirana <i>et al.</i> (2014)	1989-2008	2208	1188	1033	0.54	0.47	-13
Carmona (2015)	1982-2008	2266	1163	1189	0.51	0.52	-86
Builes-Jaramillo and Poveda (2018)	1984-2007	2225	965	1248	0.43	0.56	12

This chapter reviews the main features and the main large-scale and mesoscale mechanisms that cause the mean Amazon climate, its interannual and interdecadal variability, and extreme drought and flood events (Sections 5.2 and 5.3). The effects of extreme events on vegetation dynamics are discussed in Section 5.3. Next, the chapter describes the partitioning of precipitation into evapotranspi-

ration (Section 5.4), runoff, flow seasonality, and floodplain dynamics (Section 5.5). Finally, the role of floodplains in biogeochemical cycles is discussed in Section 5.6.

This chapter's description of the Amazon's physical hydroclimate system also serves as an introduction to the biosphere-atmosphere interactions discussed in Chapters 6 and 7, and to climate change as discussed in Chapter 22. Chapter 6 discusses the influence of the physical hydroclimate system on biogeochemical cycles, whereas Chapter 7 presents the rainforest's role in the water and energy exchange of this coupled biosphere-atmosphere system. Chapter 22 presents the long-term variability and changes in temperature and hydro-meteorology in the Amazon.

5.2 Main features of the Amazon climate

5.2.1 Spatial distribution of climate variables

5.2.1.1 Air temperature Due to high, relatively constant incoming solar radiation, air temperature in the Amazon is practically isothermal, with only a small variation throughout the year except in the southern part (Rondônia, Mato Grosso, Bolivian Amazon, and the Southern Peruvian Amazon). Annual averages show very high temperatures in the central equatorial region, exceeding 27-29°C. The seasonal thermal amplitude is 1-2°C, and average values range from 24°C to 26°C. The city of Belém (PA) has a maximum monthly average temperature of 26.5°C in November, and a minimum of 25.4°C in March, while Manaus (AM) has its temperature extremes in September (27.9°C) and April (25.8°C). In austral winter, the cold air masses that produce frosts in the South and Southeast of Brazil can also cool the southern and western Amazon, with significant air temperature drops (Ricarte and Herdies 2014, Viana and Herdies 2018). Near the Andes, the maximum monthly mean temperature in Santa Cruz de la Sierra, Bolivia, reaches 26.1°C in September and 20°C in June. Despite small seasonal fluctuations, large temperature oscillations (high amplitude) are typical of the diurnal cycle in this region, in association with the timing of local rainfall.

5.2.1.2 *Atmospheric circulation* The mean atmospheric circulation in the Amazon is forced by the annual cycle of solar radiation. The atmospheric circulation's main features are described here, while the solar forcing is described in Section 5.3.2. Near the Amazon delta, maximum rainfall is observed during austral summer-fall, and dry conditions prevail during wintertime (Figure 5.1). This is due to the alternating warming of the two hemispheres and to the annual cycle associated with the seasonal meridional migration of the Intertropical Convergence Zone (ITCZ) (Vera *et al.* 2006a). The trade winds coming from the tropical North and South Atlantic converge along the ITCZ and are as-

sociated with subtropical anticyclones in the North and South Atlantic.

Monsoonal rain over the Amazon Basin during austral summer provides moisture to establish an active South Atlantic Convergence Zone (SACZ; Figure 5.1). The SACZ is characterized by a convective band that extends northwest-southeast from the Amazon Basin to the subtropical South Atlantic Ocean. It is identifiable by persistent cloudiness and frequently configured in the austral summertime (Ambrizzi and Ferraz 2015). The SACZ's northern edge merges with the Atlantic ITCZ (Cai *et al.* 2020). Diabatic heating in the Amazon Basin con-

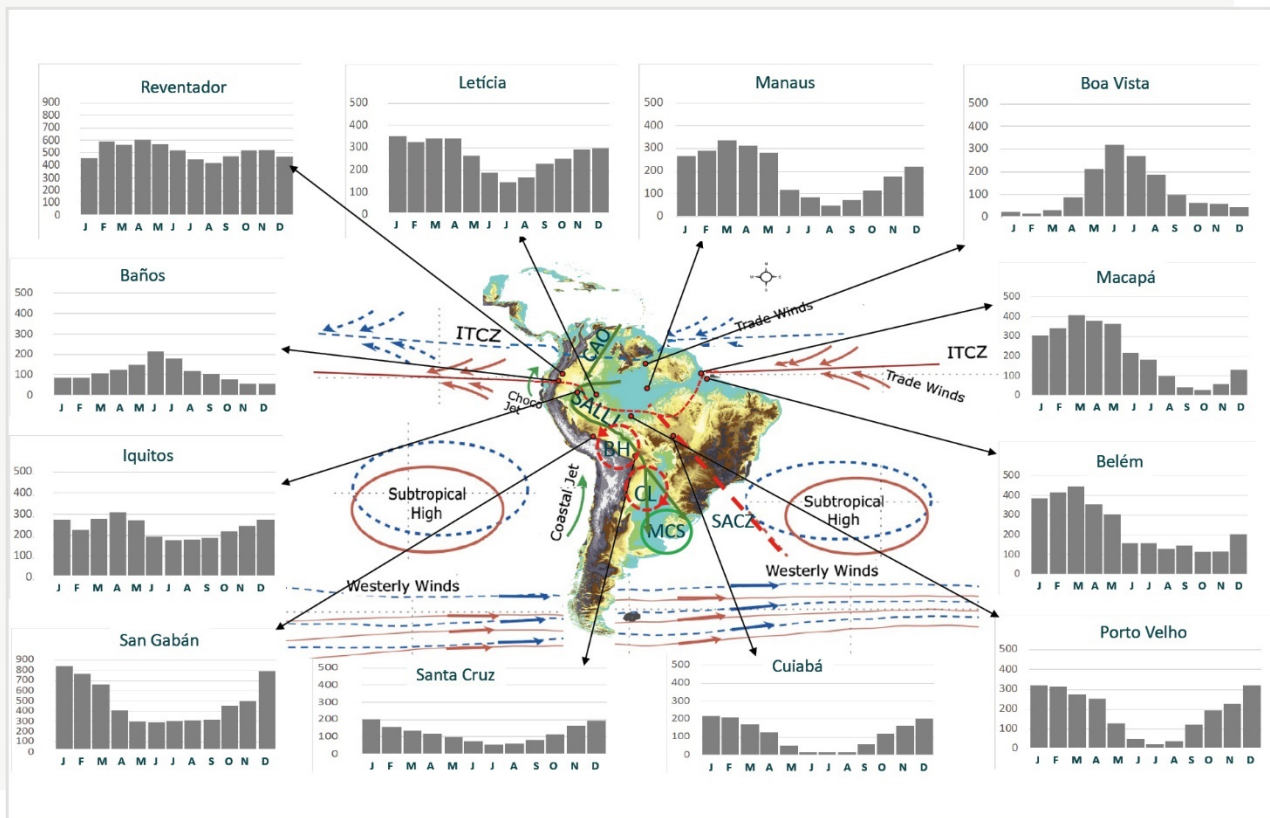


Figure 5.1 Schematic of the main climatological features in South America. The blue and red lines represent June-July-August (JJA) and December-January-February (DJF), respectively. The annual cycle of rainfall (bars) is shown for stations located in various sections of the Amazon region (in mm), indicated by dots. Low-level circulation features: CL, Chaco Low; BH, Bolivian High; ITCZ, Intertropical Convergence Zone; MCS, mesoscale convective system; SACZ, South Atlantic Convergence Zone; SALLJ, South American low-level jet. Sources of rainfall data: INMET and ANA (Brazil), SENAMHI (Peru), SENAMHI (Bolivia) and INAMHI (Ecuador). The figure is adapted from Figure 1 of Cai *et al.* (2020). Climatology is for the period 1961-2010.

tributes to the formation of the Bolivian High (BH) in the upper atmosphere (Lenters and Cook 1997). At the regional scale, moisture transport in and out of the Amazon Basin is critical for the rainfall regime, particularly during the wet season. The moisture from the Amazon is exported out of the region, transported via the South American Low-Level Jet (SALLJ) east of the Andes, interacting with the Chaco Low (CL) and contributing to precipitation over the La Plata Basin by intensifying mesoscale convective systems (Marengo *et al.* 2004, Drumond *et al.* 2008, 2014; Arraut *et al.* 2012; Vera *et al.* 2006b, Liebmann and Mechoso 2011, Jones and Carvalho 2018, Gimeno *et al.* 2016, 2020, Jones 2019, Cai *et al.* 2020).

5.2.1.3 Rainfall Because it extends into both hemispheres, the Amazon is characterized by several rainfall regimes due to the alternating warming of each hemisphere. During a ‘normal’ year, rainfall in the region shows opposing phases between the northern and southern tropics, with a rainy season in austral winter in the north and austral summer in the south. In the southern Amazon, rainfall peaks during austral summer; in the central Amazon and near the Amazon delta, it peaks in austral autumn; and north of the Equator, it peaks in austral winter (Figure 5.1). The northwest equatorial region experiences low rainfall seasonality, with wet conditions throughout the year. For more details about rainfall regimes in the Amazon Basin, see Figueroa and Nobre (1990), Rao and Hada (1990), Rao *et al.* (2016), Espinoza *et al.* (2009a, 2015), Debortoli *et al.* (2015), Marengo and Espinoza (2016), and Cai *et al.* (2020).

The onset and demise of the rainy season in the Amazon varies gradually from south to north. The end of the rainy season is more regular than its onset. The rainy season in the southern Amazon ends in April, while in the north it ends in September. SST anomalies in the Pacific or Tropical Atlantic play a dynamic role in controlling the beginning and end of the rainy season (Liebmann and Marengo 2001, Liebmann *et al.* 2007; Arias *et al.* 2015).

5.2.2 The role of ENSO and other large-scale mechanisms

5.2.1.1 ENSO The El Niño-Southern Oscillation (ENSO) is the main cause of global interannual variability in the water and energy budgets. ENSO extremes represent a reversal of the typical SST patterns in the Tropical Pacific – El Niño (EN)/La Niña (LN), when there is warming/cooling in the eastern or central-eastern tropical Pacific. EN is typically (but not exclusively) accompanied by drought in the Amazon region. In general, recent severe droughts over the Amazon have resulted in low river water levels, a high risk of forest fires, and impacts on natural river ecosystems (Cai *et al.* 2020).

Changes to atmospheric circulation during EN and drought have been summarized by Builes-Jaramillo *et al.* (2018a) and Jiménez-Muñoz *et al.* (2019). Observed anomalies in the vertical distribution of zonal and meridional wind are consistent with SST anomalies. During drought and EN years, subsidence anomalies appear over areas with negative rainfall differences over the Amazon, with convection and intense rainfall over warm SST in the eastern Equatorial Pacific region. The upper-level convergence anomalies observed during drought years over tropical equatorial South America (east of the Andes) are consistent with low-level subsidence anomalies. This suggests anomalies in the upper and lower branches of the Hadley circulation over tropical South America east of the Andes, and of the Walker circulation over the equatorial Atlantic. The ascending branch of the Walker circulation over the eastern central Pacific is the main driver of the subsidence branch over the Amazon Basin east of the Andes, which extends all the way to the tropical Atlantic.

There are different “types” of EN depending on the location of maximum warm anomalies over the tropical Pacific, Eastern Pacific (EP) EN or Central Pacific (CP) EN (Takahashi *et al.* 2011). Because the Hadley and Walker circulations are affected differently during EP-EN and CP-EN episodes (Zheleznova and Gushchina 2017), they lead to different precipitation anomalies over South America

(Tedeschi and Collins 2017; Sulca *et al.* 2018). Physical mechanisms behind the different patterns of rainfall deficits during CP- and EP-ENs and warm Tropical Northern Atlantic Index (TNA) events are described in Jiménez-Muñoz *et al.* (2019). EP-EN years were detected in 1983 and 1998, whereas CP-EN occurred in 2010 and 2016 (Sulca *et al.* 2018; Gu and Adler 2019, Gloor *et al.* 2013, 2018).

5.2.2.2 PDO, AMO, MJO In addition to ENSO, there are two other modes of interannual and interdecadal variability with teleconnections that influence the climate of the Amazon, The Pacific Decadal Oscillation (PDO) and the Atlantic Multidecadal Oscillation (AMO). They represent changes in the organization of air-sea interactions that vary at decadal scales and affect the sea surface, inducing later circulation and rainfall changes in the Amazon. For a detailed definition of these modes of variability, please see the Glossary.

Consistent with the ENSO (EN) positive phase, the PDO and AMO's positive phases matched the intensification of negative rainfall anomalies in the Amazon towards the end of 2015, during the 2015-16 EN event (Aragão *et al.* 2018). This finding is consistent with previous work (Kayano and Capistrano, 2014) showing that the Atlantic Multidecadal Oscillation (AMO) and ENSO influence South American rainfall at the end of the year, before the peak of EN.

Positive phases of the PDO are associated with an increase in precipitation in the central and northern parts of the basin and a decrease in the southern regions (Gloor *et al.* 2013). Andreoli and Kayano (2005) show that EN effects on rainfall over South America differ from those of the PDO phases in the Amazon. For example, they show negative precipitation anomalies for the warm PDO regime, consistent with the descending motion and cyclonic circulation over northern South America and the adjacent Atlantic sector. On the other hand, the relatively weaker circulation patterns in these sectors result in smaller magnitude precipitation anomalies in the Amazon for the cold PDO phase.

The intraseasonal variability is particularly important during the austral winter (Mayta *et al.* 2018). Previously, Souza and Ambrizzi (2006) found that the Madden-Julian Oscillation (MJO) is the main atmospheric mechanism influencing rainfall variability at intraseasonal timescales over the eastern Amazon and during the rainy season in northeast Brazil. During the drought of 2005, however, the intraseasonal oscillation was weaker than normal, favoring drought conditions in the region. The Tropical North Atlantic played a major role in this drought (Builes-Jaramillo *et al.*, 2018b).

5.2.3. Extreme drought and flood events

In the last 15 years, the Amazon Basin has witnessed climate extremes, some of them characterized as 'events of the century'; droughts in 2005, 2010, and 2015–16; and floods in 2009, 2012, 2014, and 2021. Historical records show previous droughts in 1926, 1964, 1980, 1983, and 1998; and floods in 1953, 1988, 1989, and 1999. These events have been linked to modes of natural climate variability (EN, warm TNA anomalies) with strong impacts on natural and human systems. Some of the Amazon's main cities were flooded during flood years or isolated by extremely low river levels during droughts. The number of fires increased during drought years, releasing carbon, smoke, and soot into the atmosphere and affecting the local population (Marengo and Espinoza 2016, Gatti *et al.* 2014, Aragão *et al.* 2018, Jiménez-Muñoz *et al.* 2016, 2019). The year 1999 and other wet years (1988-89, 2007-2008, and 2011-2012) were LN years (see Chapter 22). It is worth mentioning that droughts and floods are not synchronous and do not affect the whole basin in the same way, as seen in Figures 5.2 and 5.3.

Overall, droughts affect the north-central Amazon, but the spatial pattern differs from one EN event to another and even from one drought case to another (Figure 5.2). Droughts in the Amazon have been related to EN events, such as in 1912, 1926, 1983, 1997–1998, and 2015-16 (e.g., Aceituno 1988; Williams *et al.* 2005, Coelho *et al.* 2013, Marengo *et al.* 2018, Jiménez-Muñoz *et al.* 2018, 2019). However,

the 1964 and 2005 severe droughts were exceptions, indicating TNA's active influence on those extremes (Marengo *et al.* 2008, Zeng *et al.*, 2008, Builes-Jaramillo *et al.*, 2018b). The 2010 extreme drought was related to the successive occurrences of an El Niño in austral summer and a very warm TNA in the boreal spring and summer (Espinoza *et al.* 2011; Marengo *et al.* 2011, Lewis *et al.* 2011, Gatti *et al.* 2014, Andreoli *et al.* 2012). Figures 5.2 and 5.3 show seasonal rainfall anomalies in South America for drought and wet years, respectively. In each case, whether EN or not, the geographical distribution of droughts may differ, affecting the southeastern, central, or northern Amazon differentially, and thus impacting the region's hydrology.

5.2.4 Andean-Amazon hydrometeorology and variability

This section focuses on the western Amazon, including the Andean part of the Amazon Basin. The region encompasses the upper Madeira Basin in Bolivia, Peru, and Brazil; the Amazonas-Solimões Basin in Peru and Ecuador; and the Japurá-Caquetá Basin in Colombia and Brazil. This region presents a wide variety of mountain climates, including humid conditions in the cloud forests, Páramos, and Yungas, and dry conditions in the highland Punas.

5.2.4.1 Seasonal patterns Seasonal rainfall cycles in the upper part of the Andean-Amazon Basins of Colombia and Ecuador follow a unimodal regime with a wet season during the boreal summer (Laraque *et al.* 2007; Arias *et al.* 2020). In these basins, river discharge peaks around May-July (e.g., Napo and Caquetá rivers in Figure 5.7), a pattern associated with the intensification of westward moisture advection from the equatorial Amazon Basin and orographic uplift forced by the Andean topography during boreal summer (Rollenbeck and Bendix 2011; Campozano *et al.* 2016).

The Andean-Amazon Basins of Ecuador exhibit a bimodal annual cycle of precipitation, with peak discharge observed around March-April and Octo-

ber-November in the upper part of the Napo, Pastaza, and Santiago Basins (Campozano *et al.* 2018) (e.g., Reventador station in Figure 5.1). Consequently, the lowlands of these intra-Andean Basins follow a bimodal annual cycle of discharge with peaks around June-July and October-November (Laraque *et al.* 2007). In these regions, less rainfall during boreal summer is associated with atmospheric subsidence that inhibits convective activity (Campozano *et al.* 2016; Segura *et al.* 2019).

In the southern tropical Andean-Amazon Basins (mainly south of 8°S), the dry season occurs in June-August and the rainy season in December-March, linked to the mature phase of the South American Monsoon System (SAMS) and the meridional movement of the ITCZ. River discharges over these basins show unimodal cycles peaking around January and March (e.g., Beni, Ucayali and Huallaga rivers in Figure 5.7; and Santa Cruz and San Gabán stations in Figure 5.1) (Espinoza *et al.* 2011; Lavado-Casimiro *et al.* 2012; Molina-Carpio *et al.* 2017). Rainfall seasonality is particularly strong in the upper and drier part of the Andean-Amazon Basins (usually above 3,000 m), where around 75% of total annual rainfall is observed between November and March (~100 mm/month), driven by upward moisture transport from the Amazon toward the mountains (Garreaud *et al.* 2009). Easterly winds in the upper troposphere (200-300 hPa) also favor moisture fluxes from the Amazon to the Andes at different time scales (Garreaud *et al.* 2009; Segura *et al.* 2020).

Most of the Amazon's Andean tributaries drain to two main rivers, the upper Madeira river (mainly from the Bolivian and southern Peruvian Amazon) and the Amazonas-Solimões river (mostly from the Peruvian and Ecuadorian Amazon) (Figure 5.7). At the Porto Velho station, the basin of the upper Madeira river spans 975,500 km², of which 23% are in the Andes. Mean annual discharge at Porto Velho is estimated at 18,300 m³/s, with peak values around 36,000 m³/s from March-April and lows around 5,000 m³/s from September-October (Molina-Carpio *et al.* 2017) (Figure 5.7). At the Tabatinga sta-

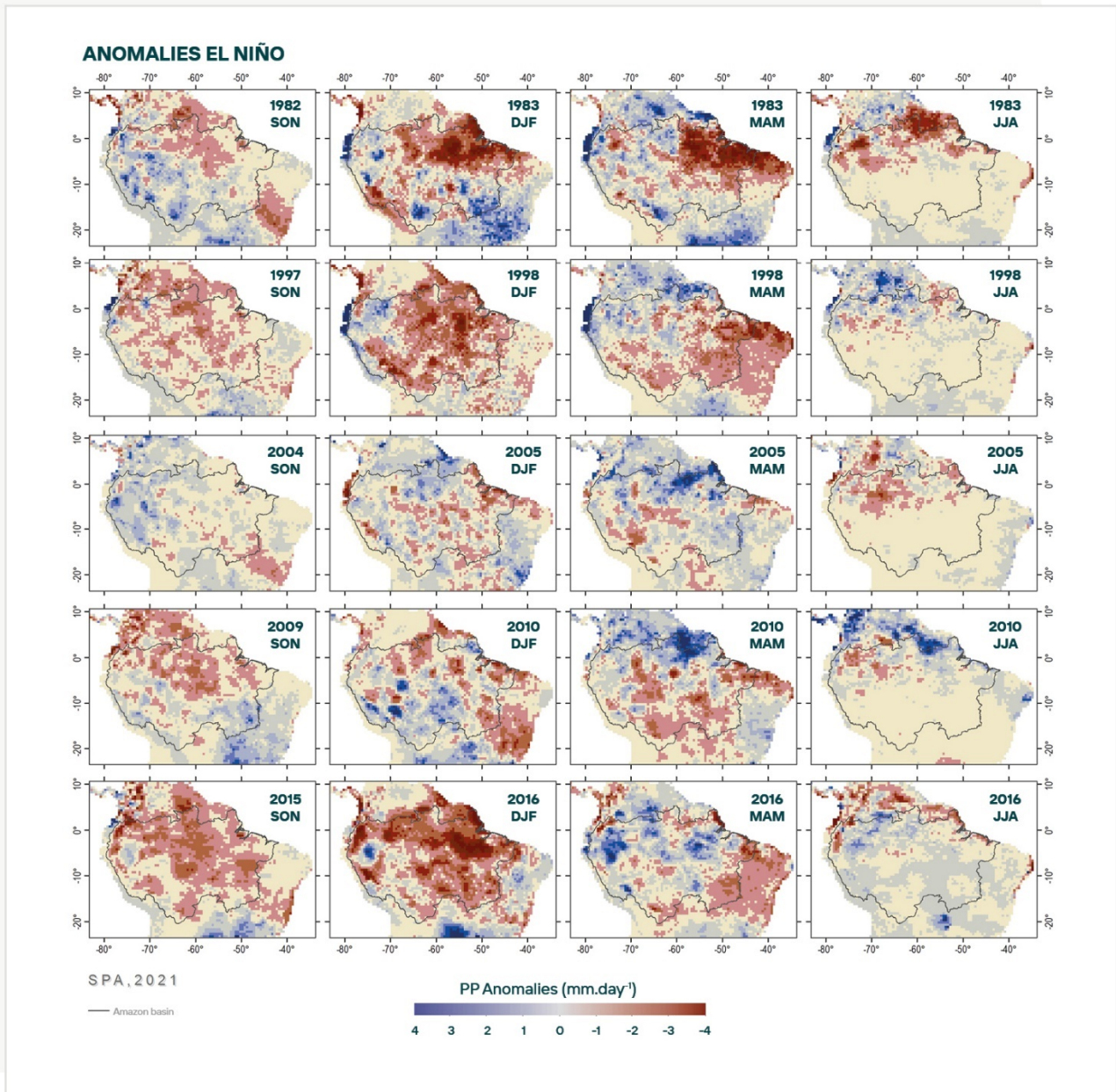


Figure 5.2 Spatial patterns of precipitation anomalies during seasons DJF, MAM, JJA, and SON for drought years in the Amazon. These are for different strong EN and TNA warming. Precipitation anomalies were obtained from the CHIRPSv2.0 dataset using the reference period 1981-2010. A black contour marks the Amazon Basin. Adapted from Jiménez-Muñoz et al. (2021; ©RMetS).

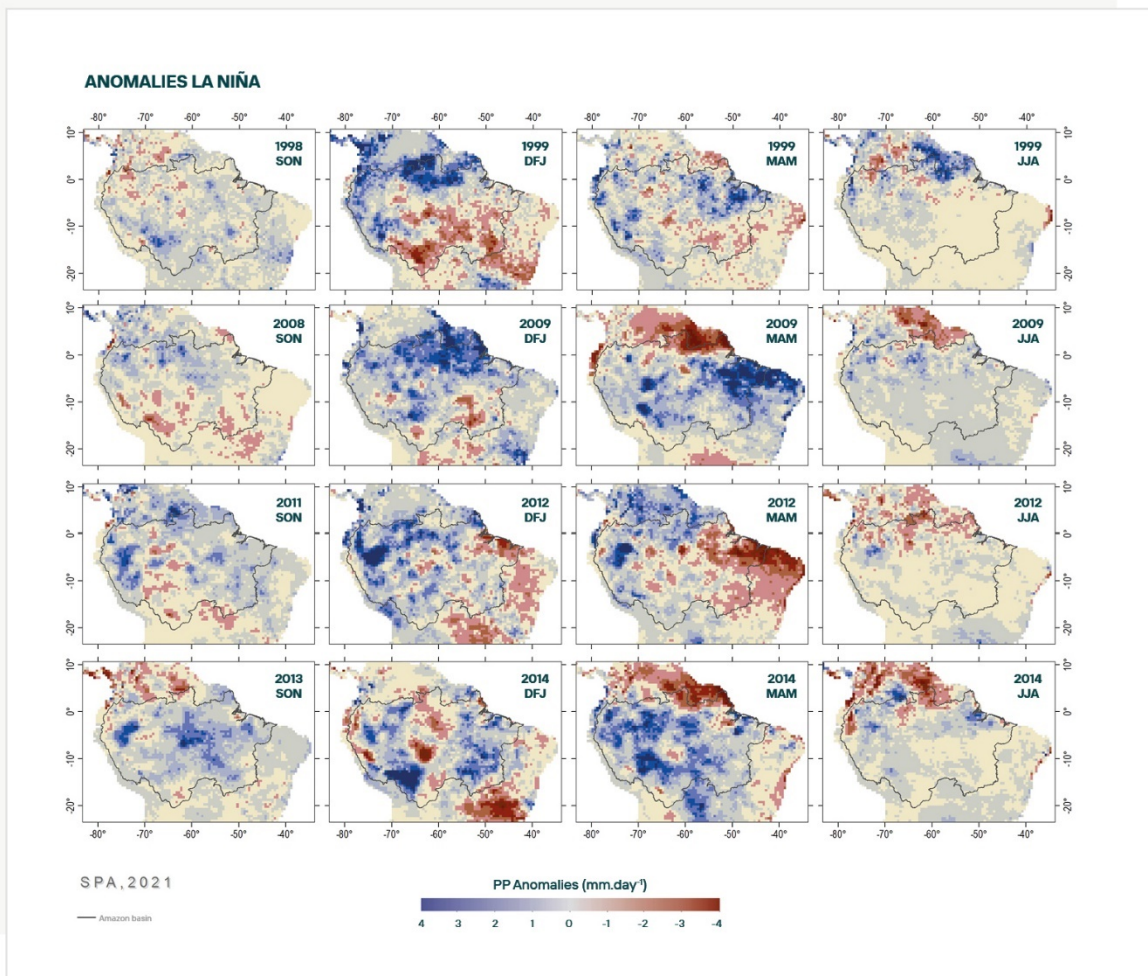


Figure 5.3. Same as in Figure 5.2 but for wet episodes (2019; ©RMetS).

tion, the Amazonas-Solimões river Basin spans 890,300 km², of which ~40% are in the Andes. The mean annual discharge at Tabatinga is estimated at 38,000 m³/s, with peak values around 51,000 m³/s from April-May and lows around 20,000 m³/s in September (Lavado-Casimiro *et al.* 2012) (Figure 5.7).

5.2.4.2 Interannual variability and extremes In the Andean-Amazon region, a rainfall deficit (excess) during austral summer is frequently associated with El Niño (La Niña) events (Poveda *et al.* 2006; Espinoza *et al.* 2011). However, different patterns occur in the upper and lower parts of the Andean-

Amazon Basins (Arango-Rueda and Poveda 2019). Recent studies have also reported different precipitation anomalies for the Central-Pacific and Eastern-Pacific El Niño types (Lavado-Casimiro and Espinoza 2014; Sulca *et al.* 2018; Navarro-Monterroza 2019). In general, the Central-Pacific El Niño (La Niña) is associated with rainfall deficits (excesses) in the upper part of the basin (the Andean regions of Colombia, Ecuador, and Peru). These anomalies are weaker during Eastern-Pacific El Niño (La Niña) events. In contrast, in the upper Madeira Basin rainfall anomalies are stronger during the Eastern-Pacific El Niño.

On seasonal timescales, rainfall anomalies over the Andean Amazon Basin range from ± 0.5 to ± 2.0 mm/day and can persist over periods of several months (Sulca *et al.*, 2018; Jiménez-Muñoz *et al.*, 2021). During the austral autumn, winter, and spring, rainfall anomalies over the Andean-Amazon region are mainly related to SST variability in the TNA, which is the main source of atmospheric moisture for the Andean-Amazon region (Arias *et al.* 2015; Hoyos *et al.* 2017; Poveda *et al.* 2020). Warm TNA anomalies are associated with increased precipitation in Colombia and Venezuela, related to enhanced atmospheric water vapor transport from the tropical Atlantic and the Caribbean Sea toward northern South America (e.g., Arias *et al.* 2020). In the Andean-Amazon regions of Ecuador, Peru, and Bolivia, warm conditions in the TNA are related to rainfall deficits, associated with a reduction in moisture advection from the Atlantic Ocean and enhanced atmospheric subsidence over the central and southern Amazon (Silva *et al.* 2008, Espinoza *et al.* 2019a; Jiménez-Muñoz *et al.* 2021).

As a result of rainfall anomalies, extreme hydrological events in the Andean-Amazon Basins have been associated either with El Niño/La Niña events or with SST anomalies in the TNA. The very unusual wet austral summer period of 2014, originating on the eastern slopes of the Peruvian and Bolivian Andes, was associated with warm anomalies in the western Pacific-Indian Ocean and over the subtropical South Atlantic Ocean (Espinoza *et al.* 2014). Wet conditions in the Bolivian Amazon during the 2014 austral summer were superimposed on flood waves from the main sub-basins, producing major floods in the region that same year (Ovando *et al.* 2016). This was also related to long-term atmospheric blocking systems during January and February of 2014 over southeastern Brazil, which ultimately caused the drought over São Paulo during the austral summer of 2014. In the higher part of the Amazon Basins' inter-Andean rivers, floods are frequently triggered by intense storms and/or rapid glacier melting during the austral spring-summer (Huggel *et al.* 2015).

5.3 The Amazon convection and mesoscale circulations

5.3.1 Nature of the Amazon convection

Atmospheric deep convection is typical in the tropics in association with the ascending branch of the Hadley-Walker cells. Upward motion extends from near the surface to above the 500 hPa level, reaching the level of free convection (LFC) where buoyant convection begins. At the large-scale ($>1,000$ km), seasonal changes in the thermal contrast between tropical South America and the Atlantic Ocean modulate wind circulation, which supplies the available energy and moist instability over the Amazon Basin (Vera *et al.* 2006a). These features provide the convective available potential energy (CAPE), gross moist instability, and rising motion essential to produce deep atmospheric convection (Garstang *et al.* 1994; Cohen *et al.* 1995; Zhou and Lau 1998). At regional (100-1,000 km) to local scales (<100 km), Amazon convection is also related to the land surface wet-bulb temperature, generally above 22°C (Eltahir and Pal 1996), which is closely determined by surface humidity and sensible and latent heat fluxes from the local land surface (Fu *et al.* 1999).

Deep atmospheric convection contributes about 80% of the total annual precipitation in the Amazon Basin, while only 20% of yearly rainfall is associated with local systems (Greco *et al.* 1990). Seasonal changes in convection are related to changes in the moistening of the planetary boundary layer (PBL) and changes in the temperature at the top of the PBL (Fu *et al.* 1999; Liebmann and Marengo 2001). However, in the northwestern Amazon, deep convection is particularly intense year-round because the warmer land surface provides a highly unstable atmospheric profile. In addition, the concave shape of the Andes induces a low-level convergence over the northwestern Amazon Basin, which is related to high annual rainfall ($>3,000$ mm) in this region (Figueroa and Nobre 1990; Espinoza *et al.* 2009b). Because deep convection over the Amazon is related to a strong release of latent heat, the Amazon basin is an important source of

energy. Through the equatorial Kelvin and Rossby waves and their interactions with the orography, the Amazon modulates the main regional structures of the atmospheric circulation in South America (Silva Dias *et al.* 1983; Figueroa *et al.* 1995; Junquas *et al.* 2015).

5.3.2 Solar forcing

Following the seasonal migration of the solar radiation maximum, the major heating zone migrates from northernmost South America (including the northern Amazon Basin) in austral winter to the central and southern Amazon in austral summer (Horel *et al.* 1989). Consequently, convective activity and rainfall enhancement show a seasonal displacement following the heating zone migration (see Section 5.2.1). Figure 5.4 shows the spatial and temporal evolution of the outgoing longwave radiation (OLR) in tropical South America, closely related to solar forcing and the development of deep convection.

The alternating warming of the two hemispheres modulates the seasonal displacement of the ITCZ,

including its Amazonian part (Figure 5.1) and the ascendant branch of the Hadley-Walker cells, which is associated with maximum rainfall over the equatorial Amazon Basin. Over this region, solar radiation peaks at the equinoxes (Figure 5.4), and the northeastern Amazon Basin displays the maximum precipitation in the austral autumn, with peaks in April and May. However, in some western equatorial Amazon regions, the wet season occurs during austral fall and spring (see Section 5.2.1). In austral spring, surface heating by solar radiation is highest over the central and southern Amazon (south of 5°S), where deep convection appears. By late November, deep convection happens over most of the Amazon Basin, mainly from 5°S to 20°S, but it is still absent over the eastern Amazon Basin and northeast Brazil (Horel *et al.* 1989; Zhou and Lau 1998).

At the peak of austral summer, following the southward migration of the sun, heating and convective activity moves toward the subtropical highlands. Rainfall peaks over the central Andes and the southern Amazon Basin during this season. The thermal contrast between the continent determin-

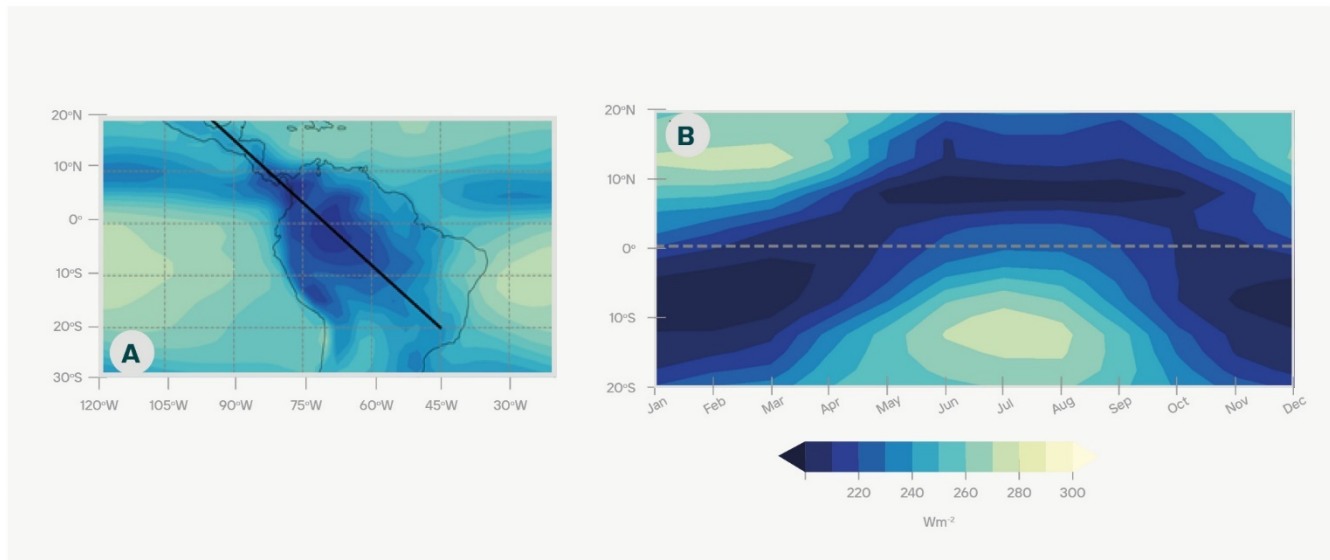


Figure 5.4 (A) 1974-2019 mean annual values of outgoing longwave radiation (OLR, in $\text{W}\cdot\text{m}^{-2}$) over tropical South America. (B) Time-latitude diagram of the climatology of monthly OLR (1974-2019) averaged across a 10° longitudinal strip centered on the black line over tropical South America shown in (a). Adapted from Horel *et al.* (1989). Interpolated OLR data provided by the NOAA/OAR/ESRL PSL ([HTTPS://PSL.NOAA.GOV](https://psl.noaa.gov); Liebman and Smith 1996).

es the SAMS configuration (Marengo *et al.* 2012). The mature phase of the SAMS (typically from late November to late February) exhibits four dominant features (Section 5.2.1 and Figure 5.1): (i) an anticyclone located over Bolivia at 200–300 hPa (the Bolivian High -BH); (ii) the occurrence of high surface temperatures over the Atlantic Ocean before the wet season begins in the southern Amazon; (iii) a northwest-southeast oriented band of maximum cloudiness over the southeast of the continent, the SACZ; and (iv) the intensification of the SALLJ to the east of the Andes (see review in Espinoza *et al.* 2020).

5.3.3 Forest breeze and river breeze circulations

Forest and river breezes are mesoscale (10-100

km) circulations close to large rivers. They result from differences in the sensible and latent heat fluxes between the hot land and the cool water during the daytime, which produces a horizontal pressure contrast. This mechanism enhances cloudiness over land during the day, while clear skies predominate over water. The opposite occurs during the night. In the Amazon Basin, convergence zones lead to enhanced rainfall over forests away from large rivers, and convective activity is reduced near rivers (e.g., Paiva *et al.* 2011; Figure 5.5).

Several studies have described river breezes in the central Amazon, using both observed and modeling approaches (e.g., Ribeiro and Adis 1984; Garstang and Fitzjarrald 1999; Cutrim *et al.* 2000). Near the Amazon-Tapajós confluence (Figure 5.5),

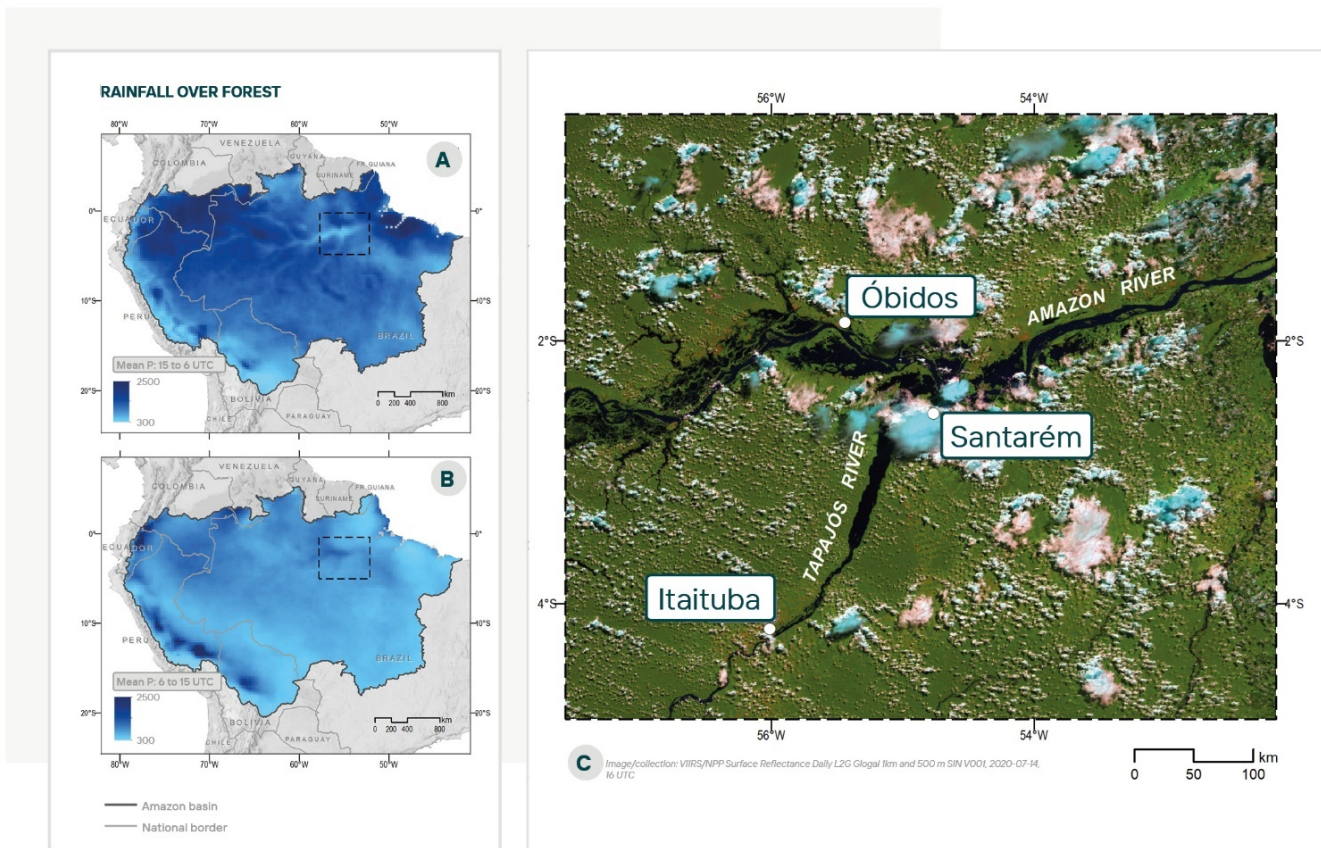


Figure 5.5 Rainfall estimated by TRMM 3B42 between (A) 15 to 06 UTC; and (B) 06 and 15 UTC. Adapted from Paiva *et al.* (2011). (c) Image of the VIIRS sensor (Visible/Infrared Imager Radiometer Suite) in true color corresponding to July 14 2020 at 16:48 UTC over the confluence of the Tapajós and Amazon rivers (dotted black box in a and b). By the NOAA/OAR/ESRL PSL (<https://psl.noaa.gov>; Liebman and Smith 1996).

rain gauges close to large rivers show less convective rainfall in the afternoon. Still, this deficit is more than compensated by additional nocturnal rainfall (Fitzjarrald *et al.* 2008). Near Manaus, dos-Santos *et al.* (2014) show that river breezes and their impact on moisture transport are more evident during the dry season. The authors show that winds away from the rivers are frequent in the morning and afternoon, transporting moist air from the rivers to the city of Manaus. In contrast, winds blowing towards rivers are mainly observed at night.

River breezes affect moisture transport (Silva Dias *et al.* 2004) and local rainfall patterns. Paiva *et al.* (2011) showed a marked reduction in rainfall over the Solimões-Amazon river and along most Amazon tributaries. Since meteorological stations are often sited near large rivers (where most Amazon cities are situated), rain gauge-derived estimates of Amazon rainfall may be biased by river breezes (Silva Dias *et al.* 2004; Paiva *et al.* 2011).

5.3.4 Sea breeze and coastal circulations

The sea breeze system occurs at coastal locations due to the propagation of cool marine air towards inland areas. This system is initiated when the land surface heats faster than the sea surface (generally under relatively clear sky conditions). The thermal contrast creates a pressure gradient force directed from sea to land, causing a shallow layer of marine air to move inland (Miller *et al.* 2003).

Over the easternmost Amazon Basin, the presence of numerous bays, rivers, lakes, and the Atlantic Ocean create the ideal environment for the formation of local circulations, which modulate the regional weather and climate (Souza Filho 2005, Planchon *et al.* 2006; Germano and Oyama 2020). The main circulation patterns of the coastal and bay breezes over this region have been described elsewhere, based on observational and modeling studies (e.g., Silva Dias *et al.* 2004; Germano *et al.* 2017; Wanzeler 2018). In Belém (in the eastern Amazon Basin), the bay breeze starts in the morning and early afternoon. It is characterized by signifi-

cant changes in wind direction from south to north (Matos and Cohen 2016) and is associated with the presence of stationary cloudiness. Rainfall peaks during the April-May season coincide with the sea breeze's maximum activity, which interacts with the Atlantic Ocean's trade winds to produce storm systems known as squall lines (Kousky 1980; Silva Dias 1987; Cohen *et al.* 1995).

Squall lines are multicellular storms that propagate inland in the Amazon Basin for over 1000 km at speeds of 50–60 km h⁻¹ (Garstang *et al.* 1994; Greco *et al.* 1994). At the mesoscale, squall lines are characterized by advection of moisture produced by a sea breeze, a strong and deep low-level easterly jet, and a heat source in the central and western Amazon (Cohen *et al.* 1995). Strong jets tend to propagate the squall lines at higher speeds, with a longer lifetime and increased cloud development, forming thunderstorms with strong updrafts and downdrafts, as well as lightning. Downdrafts and lightning, in turn, cause disturbances that affect ecosystem dynamics, as described in Section 3.6.

5.3.5 Orographic-induced circulations and spatial rainfall distribution in the Andean-Amazon region

The Andean-Amazon hydrometeorology is characterized by interactions between regional atmospheric circulation, lowland-highland temperature contrast, and the complex Andean topography (e.g., Houze 2012; Roe 2005; Barry 2008). In addition, regional atmospheric circulation over South America is directly influenced by the Andean orography, particularly at low-levels (Figueroa *et al.* 1995). In the Andean-Amazon region, the SALLJ and the Llanos Jet (or *Corriente de los Andes Orientales*, CAO) are strongly controlled by the presence of the Andes, which acts like a barrier to the west, and the Amazon Basin to the east (e.g., Marengo *et al.* 2004; Jiménez-Sánchez *et al.* 2019). These LLJs are key elements of the South American atmospheric circulation because they transport vast quantities of moisture along large meridional distances throughout the east of the Andes. Indeed, the CAO's easterly flow reaches the eastern pied-

mont of the Andes as the northernmost leg of the SALLJ (Espinoza *et al.* 2020; Poveda *et al.* 2020).

At the local scale, Andean orography can influence atmospheric circulation through mechanical and thermal processes. The diurnal cycle of insolation generates thermally driven winds, such as anabatic (warm upslope) and katabatic (cold downslope) winds due to radiative warming of the surface during the day and radiative cooling during the late afternoon and night, respectively (e.g., Wallace and Hobbs 2006; Junquas *et al.* 2018). In addition, katabatic winds from the Andean highlands could trigger mesoscale convective systems (MCS) over the Andean-Amazon transition region (Trachte *et al.* 2010a,b; Kumar *et al.* 2020). Over this region, large and medium MCS are generally related to wet episodes, enhanced by the orographic lifting of moisture advection from the SALLJ (e.g., Giovannetone and Barros 2009; Romatschke and Houze 2013). Consequently, the mountainous precipitation diurnal cycle is associated with complex characteristics related to local atmospheric circulations (Poveda *et al.*, 2005; Junquas *et al.*, 2018). For example, on the eastern slopes of the tropical Andes, the highest precipitation rates are observed at night due to downslope wind and moisture transport (Figures 5.5a and b). Observational and modeling studies have shown that inter-Andean valleys also generate mechanical channelization of the moisture flux, which could contribute to moisture and rainfall over the tropical Andes, where glaciers, agriculture, and food security depend on precipitation. This includes regions such as La Paz, Cuzco, and the Mantaro valleys (Egger *et al.* 2005; Junquas *et al.* 2018; Saavedra *et al.* 2020). Convective activity forced by the Andes also generates sudden reversals of the river stage in the western Amazon (e.g., near Iquitos, Peru), where riparian agriculture is closely related to the annual hydrological cycle (Figueroa *et al.*, 2020).

Interactions between large-scale atmospheric circulation and the orographic circulations described above contribute to the high spatial variability of precipitation over the Andes-Amazon region. Studies have described a complex relationship between

altitude and rainfall, which produces a strong spatial rainfall gradient associated with the windward or leeward exposure of the rain station to the dominant moist wind (Bookhagen and Strecker 2008; Espinoza *et al.* 2009b, Rollenbeck and Bendix 2011). The highest rainfall rates in the Amazon Basin (6,000–7,000 mm/year) are generally observed at about 400–2,000 m in the Amazon Basin of Colombia, Ecuador, Peru, and Bolivia (Poveda *et al.* 2014; Espinoza *et al.* 2015; Chavez and Takahashi 2017) (e.g., San Gabán station in Figure 5.1). As a result of these rainfall characteristics, the Andean Basins show the highest runoff per unit area of the Amazon River Basin (Moquet *et al.* 2011; Builes-Jaramillo and Poveda 2018), and Andean rivers drain sediments, pollutants, and nutrients downstream to the Amazon lowlands (McClain and Naiman 2008; Vauchel *et al.* 2017). In turn, the Amazon lowlands export water vapor and nutrients to the Andes through the moisture-laden trade winds, which is part of a strong interaction between the Amazon-Andes hydroclimatic system (e.g. Staal *et al.*, 2018; Weng *et al.*, 2018, Espinoza *et al.*, 2020).

5.3.6 The role of extreme weather events on ecosystem dynamics

At least two types of extreme weather events affect ecosystem dynamics and the natural carbon cycle. First, severe storms associated with squall lines can propagate strong downdrafts (Fujita 1990, 1981, Garstang *et al.* 1998) that cause forest blow-downs (Nelson 1994, Garstang *et al.* 1998, Negrón-Juárez *et al.* 2010, Espírito-Santo *et al.* 2010), affecting forest structure and species composition (Marra *et al.* 2014, Rifai *et al.* 2016, Magnabosco Marra *et al.* 2018, Chambers *et al.* 2009). Second, lightning is a frequent disturbance mechanism that can propagate fire and kill trees directly (Gora *et al.* 2020, Yanoviak *et al.* 2020, McDowell *et al.* 2018, Foster, Knight, and Franklin 1998). The frequency of lightning is positively associated with the density of large trees and biomass stocks in tropical forests (Gora *et al.* 2020). In the Amazon, this is important in the southern and eastern transition zones between forests and savannas, but also in Roraima state (Gora *et al.* 2020).

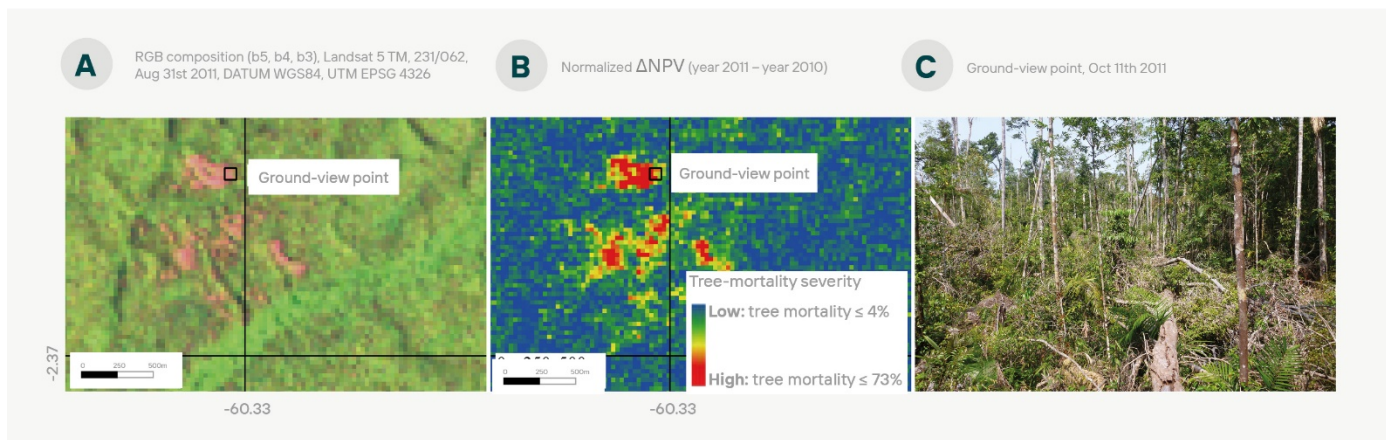


Figure 5.6 Forest blowdown (total area of ca. 91 ha) in 2011 in the Central Amazon, Brazil. Blowdowns can be identified on satellite imagery by geometric and spectral features such as defuse shape and high short-wave infrared reflectance, indicating non-photosynthetic vegetation (NPV) resulting from widespread tree damage and mortality (A). The severity of the associated tree-mortality can be estimated using normalized Δ NPV (year of the blowdown – previous year) combined with field-measured tree mortality (B). Edge of the blowdown/old-growth forest less than six months after disturbance, with toppled, survivor, and resprouting trees (C). By the NOAA/OAR/ESRL PSL (<https://psl.noaa.gov/>; Liebman and Smith 1996).

5.3.6.1 Severe storms, blowdowns, and impacts on forest ecosystem dynamics Wind is a major cause of disturbance in forests worldwide, with impacts ranging from minor loss of leaves to widespread tree-mortality (Mitchell 2013). In the Amazon, convective storms can generate strong downdraft winds and extreme rainfall (e.g., 26–41 m s⁻¹ and 30 mm h⁻¹, respectively) (Garstang *et al.* 1998; Fujita *et al.* 1990; Negrón-Juárez *et al.* 2010) that can fell forest patches ranging in size from <2 ha (Negrón-Juárez *et al.* 2011) to >3,000 ha (Nelson *et al.* 1994). Large blowdowns can be associated with squall lines (Negrón-Juárez *et al.* 2010; Araujo *et al.* 2017). Forest blowdowns can be detected with remote sensing imagery because they create a large contrast in geometric and reflectance patterns between images acquired before and after the event (Figure 5.6A).

Blowdowns occur across the Amazon Basin, with the highest frequency in the Northwest region (Nelson *et al.* 1994; Negrón-Juárez *et al.* 2018; Espírito-Santo *et al.* 2010). In the Central Amazon near Manaus, blowdowns mostly occur during the transition from the dry to rainy season (Negrón-Juárez *et al.* 2017). The size distribution of blowdowns follows a power-law (Negrón-Juárez *et al.*

2018; Chambers *et al.* 2009), resulting in a mosaic of forest patches at different successional stages (Chambers *et al.* 2013). Because of their greater frequency, relatively small-sized patches dominate the landscape.

Tree damage and mortality occur when wind and rain loads exceed the mechanical stability of trees, leading to snapping and uprooting (Ribeiro *et al.* 2016; Peterson *et al.* 2019). In the Amazon, winds, and rain interact with different forest types that may harbor more than 280 tree species in a single hectare (de-Oliveira *et al.* 1999). In these heterogeneous forests, storm mortality can be controlled by biotic and abiotic factors (e.g., within species and across topography), with severely damaged areas experiencing up to 90% tree mortality (Maganbosco Marra *et al.* 2014; Rifai *et al.* 2016) (Figure 5.6B). The forest can lose its typical closed-canopy structure and accumulate large amounts of wood debris on the forest floor (Figure 5.6C). This gradient of gap sizes and resource/niche availability has relevant consequences for regional patterns of forest dynamics, biodiversity, and biogeochemical cycles.

Tree mortality can be selective and depends on species traits and individual characteristics (Ribeiro *et al.* 2016; Magnabosco *et al.* 2014; Rifai *et al.* 2016). Snapping and uprooting of large individual trees can topple neighbors, altering the number and size distribution of trees and reducing stand biomass. Mortality rates among surviving trees are higher in the first years following the event, slowing biomass recovery. Resprouting and growth of survivor trees contribute little to biomass recovery, which can take decades (Magnabosco Marra *et al.* 2018). Recovery trajectories differ with the severity of mortality. However, even low severities trigger secondary succession, with substantial species turnover and dynamics distinct from those observed in small treefall gaps and human forest clearing (Chambers *et al.* 2009b; Magnabosco Marra *et al.* 2014, 2018). Soil organic carbon can also increase as a function of blowdown severity due to the decomposing organic matter available from wood debris (dos-Santos *et al.* 2016).

Blowdowns can also promote tree diversity by providing niches to a diverse cohort of species that differ widely in their requirements and recruitment strategies (Magnabosco *et al.* 2014; Chambers *et al.* 2009). Nonetheless, altered functional composition indicates that blowdowns may affect the resilience of biomass stocks by favoring soft-wooded species with shorter life spans, which are also more vulnerable to future disturbances (Magnabosco Marra *et al.* 2018; Trumbore *et al.* 2015). The impacts of blowdowns can be more pronounced in secondary and fragmented forests with altered composition and structure, and a relatively higher proportion of exposed edges (Silvério *et al.* 2019; Schwartz *et al.* 2017). That aspect is critical since these account for large areas of the remnant forests in highly deforested regions of the Amazon (Brando *et al.* 2014; Hansen *et al.* 2013).

Research has focused on detecting blowdowns and quantifying their local to regional impacts on species composition, and forest structure and dynamics. However, the effects of blowdowns on forest functioning at the landscape scale are still poorly understood. Assessing the return frequency of dis-

turbances and the recovery rates of biomass and functional composition in different regions is critical to understanding variations in carbon balance at broader spatial scales. Climate change projections indicate that the frequency and intensity of convective storms could increase in the Amazon (Negrón-Juárez *et al.* 2017; McDowell *et al.* 2018; IPCC Climate Change 2014). Determining the possible thresholds of disturbance severity under these shifting disturbance regimes is thus critical, since it will affect the future vulnerability and resilience of the Amazon forest (Trumbore *et al.* 2015; Turner *et al.* 2010). The effects of forest blowdowns on other taxa remain unassessed in the Amazon.

5.3.6.2 Lightning, natural fires, and impacts on vegetation structure and biome distribution Lightning is an impressive and common phenomenon in the Amazon due to the meteorological systems that occur there, such as the squall lines and the SACZ. Natural fires can happen when electrical storms develop in conditions where vegetation is dry, especially when cloud-to-ground lightning is accompanied by little precipitation (conventionally ≤ 2.5 mm) (Viegas 2012; Nauslar *et al.* 2013). This phenomenon, known as “dry lightning” or “dry thunderstorm”, also happens when the rain evaporates before reaching the ground, if a storm moves quickly, or if cloud-to-ground lightning occurs outside the region where precipitation occurs (Dowdy and Mills 2012).

Natural causes have been reported as important for ignition in the Cerrado, mainly due to cloud-to-ground lightning during the transition between dry and rainy seasons (Ramos-Neto and Pivello 2000). There is still no conclusive information on the proportion of human versus natural causes, but natural fires are believed to be around 1-2% of total fires (Alvarado *et al.* 2018).

The transition between the Amazon and Cerrado in Brazil has the largest area of contact between forest and savanna in the tropics, and these biomes differ fundamentally in their structural characteristics and species composition (Torello-Raventos *et al.* 2013). In this transition, rainfall seasonality and

fire disturbances have an important ecological effect on the vegetation structure and composition due to influences on the ecological and biogeochemical processes of vegetation directly affecting the Net Primary Production and respiration that, over time, lead to changes in composition and structure of vegetation (Alves *et al.* 1997). Fires change plants' phenology and physiology, modify competition among trees, and lower canopy plants such as grasses, shrubs, and lianas. Depending on its frequency and intensity, fire may increase trees' mortality and transform an undisturbed forest into a disturbed and flammable one (House *et al.* 2003; Hirota *et al.* 2010; Hoffmann *et al.* 2012). Tree species associated with forest or savanna vegetation differ in numerous physiological characteristics, such as fire survivorship (Hoffmann *et al.* 2009; Ratnam *et al.* 2011) and their wood and foliar characteristics (Gotsch *et al.* 2010).

Couto-Santos *et al.* (2014) demonstrated the effects of climate variability and fire occurrence on forest-savanna boundaries in Roraima, in the northern part of the Brazilian Amazon. In wet years, the forest advanced over the savannas, while in years with lower rainfall, the forest receded, and the savanna expanded due to the increased frequency of drought and fire.

5.4 Evapotranspiration

When rainwater reaches the rainforest's land surface, most of it infiltrates into the soil, increasing soil moisture. About 50% of the rainfall returns to the atmosphere as evapotranspiration (ET: plant transpiration plus water evaporation from free water surfaces and bare soil; see Table 1). The remainder supplies the groundwater pool, which ultimately contributes to the formation of the Amazon Basin's streams and rivers. This section discusses the seasonal patterns of ET and their controlling mechanisms. The role of ET as a source of water to the atmosphere, and consequently for the processes of rain formation, is discussed in Chapter 7.

An early attempt to characterize Amazonian ET was made during the Amazon Region Micromete-

orological Experiment (ARME), a British-Brazilian experiment. Starting in 1983, this campaign made several micrometeorological measurements at the Ducke Reserve, about 30 km northeast of Manaus. Using ARME's data and the Penman-Monteith equation, Shuttleworth (1988) showed a small seasonality in ET, with peaks in March and September that coincided with net radiation (Rn) extremes. The study also found that actual ET rates were nearly equal to potential ET rates throughout the year, suggesting plenty of water availability even during dry periods.

Starting in the late 1990s, during the Large-Scale Biosphere-Atmosphere project (LBA), a network of intensive eddy-covariance (EC) measurements was set up throughout the lowland Amazon to quantify surface energy, water, and carbon fluxes under different land covers (Keller *et al.* 2004). Data analysis from the EC flux towers revealed different ET seasonality depending on the study site. Most of the sites showed a seasonal pattern similar to that observed at Manaus during ARME – i.e., ET in phase with Rn, maintaining either a constant flux or showing a slight increase during the dry period compared with the rainy season (Costa *et al.*, 2004; Hutyrá *et al.* 2005; Juárez *et al.* 2007; da Rocha *et al.* 2004; Sommer *et al.* 2003; Souza-Filho *et al.* 2005; Vourlitis *et al.* 2002). A few studies, mostly located in the Southwestern Amazon (Aguiar *et al.* 2006) or at the transition between Amazon forests and cerrado savannas (Borma *et al.* 2009), observed higher ET in the rainy season compared with the dry season.

Syntheses of flux tower observations across the Amazon (Costa *et al.* 2010; Hasler and Avissar 2007; Juárez *et al.* 2007), comparisons of the Amazon with other biomes (da Rocha *et al.* 2009), and a pan-tropical analysis (Fisher *et al.* 2009) helped elucidate the seasonal and spatial variability of Amazonian ET. Hasler and Avissar (2007) found strong seasonality in ET for the stations near the equator (2°S-3°S), with ET increasing during dry periods (June-September) and decreasing during wet periods (December-March), both correlated and in phase with Rn. In stations located further south

(9°S-11°S), ET and Rn did not present clear seasonality. These studies found the best correlations between ET and Rn at these sites during wet periods, but no correlation during dry periods. The authors attributed this response to water stress during dry periods, especially at the drier southern sites.

Negron-Juarez *et al.* (2007) analyzed ten LBA sites and concluded that all of them had higher ET during the dry period than during the rainy period. Fisher *et al.* (2009) analyzed 21 pan-tropical sites and observed an increase in ET in the dry period compared to the rainy period, with Rn explaining 87% of monthly ET variance. Da Rocha *et al.* (2009) analyzed ET data from EC flux towers at seven sites, four of them located in the northern Amazon Basin and three in the Cerrado (semideciduous forest, transitional forest floodplain, and cerrado). They observed that the seven sites analyzed could be divided into two functional groups in terms of ET seasonality. The southernmost sites, generally drier and with a longer dry season, showed decreased ET in the dry period compared to the rainy period. Minimum ET values of 2.5 mm/day were observed in transitional forests, and a minimum of 1 mm/day was observed in the cerrado sites. The northern and more humid sites, with dry season length under four months, showed the opposite pattern, with increased ET in the dry season and maximum values of around 4 mm/day. ET, Rn, and vapor pressure deficit (VPD) were positively correlated at these sites, suggesting that atmospheric conditions exert control over ET. However, it is important to consider that the most seasonal sites studied by da Rocha *et al.* (2009) had a predominance of deciduous and semi-deciduous vegetation. In these sites, the falling leaves in the dry period may have exercised important controls over ET, together with climatic conditions.

Costa *et al.* (2010) analyzed three evergreen rainforest wet equatorial sites (2°S-3°S) and two seasonally dry rainforest sites (at about 11°S). They observed that, in general, dry season ET is greater than rainy season ET. Following previous studies, they found that Rn was the main controlling factor

of ET in wetter sites, followed by VPD and aerodynamic resistance. They identified different controlling factors of ET in wet and seasonally dry sites. While ET seasonality in humid equatorial forests was controlled only by environmental factors (i.e., abiotic controls), in seasonally dry forests ET was controlled by biotic parameters (e.g. stomatal conductance, g_s), with surface conductance varying by a factor of two between seasons.

Observational studies generally agree on the seasonal pattern of ET in the Amazon rainforest, where ET is strongly dependent on net radiation (Rn) for seasonally humid forests. In the early 2000s, however, most models still simulated ET as being in phase with precipitation (Bonan 1998; Werth and Avissar 2004; Dickinson *et al.* 2006), suggesting that water availability limits ET. Around 2010, the LBA Data-Model Intercomparison Project (LBA-DMIP) compared the results of 21 land surface and terrestrial ecosystem models to the comprehensive observational dataset from the LBA network of flux towers to evaluate how well the new generation of models could reproduce the Amazon rainforest and Cerrado functions (de Gonçalves *et al.* 2013). As part of this project, Christoffersen *et al.* (2014) concluded that models have improved in their capacity to simulate the magnitude and seasonality of ET in equatorial tropical forests, having eliminated most dry-season water limitation. Their performance diverges in transitional forests, where seasonal water deficits are greater, but mostly capture the observed seasonal depressions in ET seen in the Cerrado. Many models depended only on deep roots or groundwater to mitigate dry season water deficits. Some models were able to match the observed ET seasonality, although they simulated no seasonality in stomatal conductance (g_s). Some of these deficiencies can be improved by parameter tuning, but in most models these findings highlight the need for continuous process development (Christoffersen *et al.* 2014).

In summary, ET is controlled by the balance between water demand imposed by the atmosphere (aboveground conditions) and the water supply in

the soil (belowground conditions). Both are considered abiotic controls (Costa *et al.*, 2010) or ecohydrological mechanisms (Christoffersen *et al.* 2014). By opening and closing stomata, plants may exercise important additional controls over evapotranspiration fluxes through stomatal canopy conductance (Costa *et al.* 2010; Christoffersen *et al.* 2014), resulting in a balance between photosynthesis and transpiration (Beer *et al.* 2009; Lloyd *et al.* 2009). These biotic (Costa *et al.*, 2010) or ecophysiological (Christoffersen *et al.* 2014) control mechanisms over ET and their importance in the context of regional climate will be discussed in detail in Chapter 7 (Section 7.2.2).

5.5 Main characteristics of the surface hydrological systems in the Amazon

The Amazon River Basin (including the Tocantins River as a tributary and other coastal basins) drains about 7.3 million km² and discharges about 16-22% of all global river inputs to the oceans (Richey *et al.* 1989; see also Box 5.1). This vast hydrological system is formed by the Andes, the Guiana and Brazilian shields, and the Amazon plain (Sorribas *et al.* 2016). As a consequence of the seasonal rainfall cycle (Section 5.2.2), the main stem Amazon River and its tributaries exhibit high and low river levels a few months after the preceding wet and dry seasons.

In general, rivers in the southern Amazon Basin (e.g., Solimões, Madeira, Xingu, Tapajós, Tocantins-Araguaia) peak from April–May, whereas rivers in the northern Amazon (e.g., Japura-Caquetá, Rio Negro) peak from May–June (Espinoza *et al.* 2009a, b, Marengo and Espinoza *et al.* 2016). At annual time scales, the hydrological contribution of southern and northern rivers is roughly equivalent due to much higher total rainfall in the smaller northern basins compared to the larger southern basins.

5.5.1 Seasonality of discharge

As noted above, the discharge of the mainstem Amazon River and its tributaries integrates hydrologi-

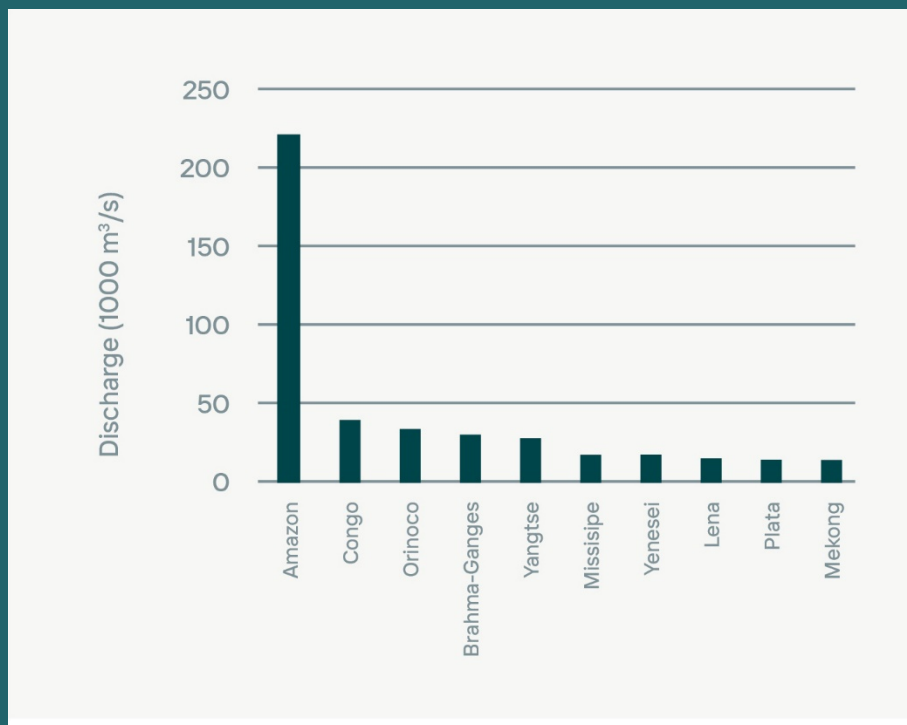
cal fluctuations occurring upstream. These hydrological dynamics show a strong a few months (See Section 5.2.2), with significant variations in the timing and magnitude of discharge across the Amazon's tributary watersheds (Sorribas *et al.* 2016). The southern and western reaches of the Amazon River usually flood first, peaking between March and May. In the central Amazon, river levels are controlled by contributions from northern and southern tributaries, generally peaking in June (Figure 5.7).

Long-term discharge measurements recorded near the central Amazon city of Óbidos, for example, indicate a peak discharge approaching ~250,000 m³s⁻¹ during the high-water period in June, and a minimum discharge of ~100,000 m³s⁻¹ during the low-water period in November (Goulding *et al.* 2003).

Because the northern headwaters of the Amazon are near the equator, their water levels fall between October and February, even as the Amazon River is rising due to contributions from the large southern tributaries. Small coastal watersheds of the northern Amazon (e.g., the Araguari) are also influenced by ocean tides in their lower reaches. In contrast, most of the Amazon River's southern tributaries reach their highest levels in March or April (at points >300 km upstream from their mouths) and their lowest levels between August and October (Goulding *et al.* 2003). For example, discharge at Itaituba in the Tapajós River peaks at ~23,000 m³s⁻¹ in March and reaches its minimum (~5,000 m³s⁻¹) in October (Figure 5.7). To its west, the Purús River at Arumã-Jusante shows even more pronounced variability, with a peak discharge of 11,000 m³s⁻¹ in April and a minimum discharge of ~1,000 m³s⁻¹ in September (Coe *et al.* 2008). The lower sections of these southern tributaries are heavily influenced by a backwater effect of the Amazon River itself, rising and falling in response to changes in the main stem (Sorribas *et al.* 2016).

BOX 5.1: How Large is the Amazon River?

“Born in the lofty, snow-clad Andes, the Amazon flows four thousand kilometers until it confronts the Atlantic at the equator. The Amazon is not only the world’s longest river; it carries more water than any other river – more than ten times that of the Mississippi, for example (**Figure B.5.1.1**). One-fifth of all the water flowing off the face of the earth passes through the Amazon’s mouth. Such is the force of the Amazon as it clashes with the Atlantic that it pushes a vast plume of freshwater for hundreds of kilometers into the sea. Five centuries ago a Spanish explorer traveling up the coast of Brazil noted that at a certain point the sea tasted fresh, even though his ship was out of sight of land. Pinzón dubbed that spot the sweet sea (mar dulce), which historians and geographers take to be the mouth of the river, named after women warriors in Greek mythology. The Southern Equatorial Current pushes this turbid plume, which reaches some 400 kilometers long and between 100 and 200 kilometers wide, in a northwesterly direction up the coast of Amapá and the neighboring Guianas. Because it is lighter, the freshwater overrides the salty oceans and dilutes and muddies the surface for up to one million square miles.” (Quoted from Smith 2002).



Most people know that the Amazon River is the largest river of the world. What most people do not realize is just how large it really is. This figure **Figure B.5.1.1** compares the world’s 10 largest rivers by discharge, showing the remarkable difference between the Amazon and all other rivers. The Amazon discharges about five times more water to the ocean than the world’s second largest river, the Congo. The magnitude of the difference is so striking that the Amazon’s largest tributary, the Madeira – discharging about 50,000 m³/s to the main stem – would rank second among the world’s largest rivers if considered independently.

A large discharge is a direct consequence of both a large drainage area and high precipitation. The Amazon ranks first in both variables, with the largest drainage area and the highest rainfall in the world.

5.5.2 Seasonality of floodplain dynamics

Fluctuations in rainfall and river discharge drive pronounced seasonal changes in the water level of large Amazon rivers, causing them to overflow their banks into adjacent floodplains. On a local scale, flooding can also result directly from rainfall in areas with poorly drained soils or rising ground-

water levels, as in the case of the Llanos de Mojos in Bolivia. The periodic rise and fall of water levels – often referred to as the seasonal flood pulse – connects rivers and their floodplains during part of the year (rivers rise between November and June, and recede between June and November), resulting in heterogeneous habitat structure, rapid recycling of nutrients and organic matter, and high rates of biological production (Junk *et al.* 2012). The Amazon River and its large tributaries are characterized by a monomodal flood pattern with an average amplitude of 10 m near Manaus, ranging from 2 to 18 m depending on the location and year (Melack and Coe 2013). The greatest annual river-level fluctuations occur in the southwestern Amazon, especially the Madeira, Purus, and Juruá Rivers, while the smallest changes happen in the east. Small (low-order) streams in the Amazon lowlands exhibit complex hydraulics, with backwater effects resulting in a less predictable polymodal hydrological regime (Piedade *et al.* 2001).

The characteristic vegetation in these flooded regions is strongly influenced by hydrological dynamics, including maximum inundation extent, flood amplitude, and the duration of the low- and high-water phases of the flood pulse. On average, the lowland rivers of the Amazon are flooded for 6–7 months out of the year, with southern tributaries flooding from January–May and northern tributaries from June to August. Conversely, the southern Amazon undergoes a pronounced dry season from August to December, which generally coincides with the low-water period. In the north, floods can last until September (Goulding *et al.* 2003). Seasonally inundated wetlands thus cover an extensive (17%) area of the lowland Amazon – estimated at 8.4×10^5 km² of the region <500 m above sea level

(Hess *et al.* 2015). About 44% of the wetland area is located in the Madeira River and Rio Negro watersheds, the Amazon's two largest tributaries (Figure 5.2). The Marañon sub-basin has the highest proportion of total area as wetland (20%), followed by the Madeira (19%) and Içá-Putumayo (17%). The Tapajós (5%) and Xingu (8%) sub-basins have the lowest proportion of wetland (Hess *et al.* 2015).

5.6 The role of rivers in biogeochemical cycles

Rivers and related aquatic systems are key ecosystems in the Amazon region. The region's underlying geology and landscape structure determine land-water connections via hydrological flow paths that influence river flow and chemistry. In disturbed systems, hydrological dynamics are strongly influenced by the type and intensity of land use, which may alter rates of runoff, infiltration of water into soils, and water chemistry. Castello and Macedo (2015), considering river systems of different orders, stressed that soil attributes (chemical, physical, and biological) and land use are the main drivers of river biogeochemistry and metabolism. In small catchments, deforestation may increase inputs of nutrients, phosphorus, and carbon to aquatic environments, dramatically changing their natural functions. For instance, studies in small catchments identified extensive growth of an aquatic herbaceous species, leading to a high concentration of dissolved organic matter and, consequently, higher decomposition and respiration rates (Deegan *et al.* 2011).

The cascade from small to larger river systems depends on the extent of deforestation, soil type, and topography. Rivers are important providers of dissolved organic matter and nutrients to the ocean. This organic matter's chemical characteristics are key in defining its role in the coastal ocean's metabolism. The Amazon River plume has a global influence. Recent data shows that 50–76% of the dissolved organic matter carried by the Amazon to the ocean is stable (Medeiros *et al.* 2015), contributing to long-term storage of terrigenous carbon and potentially adding to the deep ocean carbon pool.

The biogeochemistry of carbon in aquatic systems involves production, transformations, and connections to terrestrial systems in environments ranging from small rivers to large river-floodplains. Small rivers, which are well connected to the surrounding watershed, are strongly influenced by riparian vegetation and biota. In the case of large rivers and their flood plains, on the other hand, the processes of carbon, nitrogen, and other nutrients are intensively modulated within the aquatic system (see also Section 6.2.2).

Changes in river flow and the frequency of floods and droughts are connected to changing climate patterns (Section 5.2), as are aquatic biogeochemical cycles. Martinelli *et al.* (2010) showed a decrease in the concentration of nitrogen species (dissolved inorganic and organic nitrogen) in aquatic systems in the Amazon with increasing river flow, but also noted the effects of changing land use and increasing population density (>10 people/km²) in the region. One important driver of nutrient flow to aquatic systems is the soil parent material and chemistry. On weathered, heavily leached tropical soils, vegetation cover is a key component in the nitrogen and carbon cycles (Chapter 6). Nitrogen leaching to aquatic systems from "terra firme" may vary from 3 to 6 kg N-NO₃/ha/year with stream exports of around 4 kg-N/ha/yr (Wilcke *et al.* 2013). In contrast, in flooded areas where N is exported as dissolved NO₃ and NH₄, N exports can reach up to 12 kg-N/ha/yr. Lesack and Melack (1996) analyzed the impact of deforestation on nitrogen export to the aquatic system, finding an export of 2.7 kg N-NO₃/ha/yr for upland forests along the floodplain. After partial deforestation in the same area, measurements identified a 40% increase in nitrogen export in stream water, reaching 3.6 kg N-NO₃/ha/yr (Williams and Melack 1997).

In contrast, dissolved phosphorus export is typically low. Values reviewed by Buscardo *et al.* (2016) indicate dissolved phosphorus export in streams ranging from 0.01 kg/ha/yr in a terra-firme forest (Leopoldo *et al.* 1987) to 0.006 kg P/ha/yr in an upland forest bordering a floodplain lake (Lesack and Melack 1996). Exports were an order of magnitude

higher in a lower montane forest in Ecuador, reaching 0.6 kg/ha/yr (Wilcke *et al.* 2008).

5.7 Conclusions

The Amazon's rainfall, river flow, and flood regime exhibit considerable variability at seasonal, interannual and interdecadal scales, with extreme flood and drought events becoming more common in the last two decades. Seasonal variability is mainly controlled by solar forcing. ENSO events are a major cause of interannual variation in rainfall, flow, and floodplain extent in the Amazon Basin. Central-Pacific El Niños (La Niñas) are related to rainfall deficits (excesses) over the upper part of the basin (Andean region of Colombia, Ecuador, and Peru), but these anomalies are weaker during Eastern-Pacific El Niño (La Niña) events. During Eastern-Pacific El Niño events, rainfall anomalies are stronger in the Madeira Basin. The interannual modes of variability are modulated by interdecadal modes of the nearby oceans, such as the Pacific Decadal Oscillation and the Atlantic Multidecadal Oscillation. Moreover, extreme rainfall and flooding events are not necessarily associated with ENSO events.

Interactions between large-scale atmospheric circulation and orographic induced circulations result in high spatial variability of precipitation over the Amazon-Andean region, which may reach 7,000 mm/year – the highest rainfall levels seen anywhere in the Amazon Basin. As a result of these interactions, the Andean Basins also show the largest runoff per unit area, and Andean rivers deliver sediments, pollutants, and nutrients downstream to the Amazon lowlands.

5.8 Recommendations

- The main processes of the Amazon hydroclimate system (convection, mesoscale circulations, land surface processes) are associated with the rainforest's presence. Preserving and restoring the Amazon forest is essential to maintain these processes, which are important

locally, to the Andes, to South America, and globally.

- It is still unknown which factors drive recent accelerations in interannual climate variability, particularly given the interactions among deforestation, changes in atmospheric greenhouse gas concentrations, and natural modes of climate variability. Further research is needed to attribute the causes of this acceleration and to reduce uncertainties, helping to predict impacts and define conservation strategies.

5.9 References

- Aceituno P. 1988. On the functioning of the Southern Oscillation in the South American sector. Part II. Upper-air circulation. *J Clim* **2**: 341–55.
- Aguiar RG, Manzi AO, Priante Filho N, *et al.* 2006. Fluxos de massa e Energia em uma Floresta Tropical do Sudoeste da Amazônia.
- Alvarado ST, Silva TSF, and Archibald S. 2018. Management impacts on fire occurrence: A comparison of fire regimes of African and South American tropical savannas in different protected areas. *J Environ Manage* **218**: 79–87.
- Alves D, Soares JV, Amaral S, *et al.* 1997. Biomass of primary and secondary vegetation in Rondônia, Western Brazilian Amazon. *Glob Chang Biol* **3**: 451–61.
- Ambrizzi T and Ferraz SET. 2015. An objective criterion for determining the South Atlantic Convergence Zone. *Front Environ Sci* **3**: 23.
- Andreoli R V and Kayano MT. 2005. ENSO-related rainfall anomalies in South America and associated circulation features during warm and cold Pacific decadal oscillation regimes. *Int J Climatol A J R Meteorol Soc* **25**: 2017–30.
- Andreoli RV, Ferreira de Souza RA, Kayano MT, and Candido LA. 2012. Seasonal anomalous rainfall in the central and eastern Amazon and associated anomalous oceanic and atmospheric patterns. *Int J Climatol* **32**: 1193–205.
- Aragão LEOC, Anderson LO, Fonseca MG, *et al.* 2018. 21st Century drought-related fires counteract the decline of Amazon deforestation carbon emissions. *Nat Commun* **9**: 536.
- Arango-Ruda E and Poveda G. 2019. Efectos de El Niño y La Niña sobre la hidrología de la Amazonia colombiana. *Rev Colomb Amaz Nueva Época* **11**: 33–58.
- Araujo RF, Nelson BW, Celes CHS, and Chambers JQ. 2017. Regional distribution of large blowdown patches across Amazonia in 2005 caused by a single convective squall line. *Geophys Res Lett* **44**: 7793–8.
- Arias PA, Fu R, Vera C, and Rojas M. 2015. A correlated shortening of the North and South American monsoon seasons in the past few decades. *Clim Dyn* **45**: 3183–203.
- Arias PA, Garreaud R, Poveda G, *et al.* 2020. Hydroclimate of the Andes Part II: Hydroclimate Variability and Sub-Continental Patterns. *Front Earth Sci* **8**.
- Arraut JM, Nobre C, Barbosa HMJ, *et al.* 2012. Aerial Rivers and Lakes: Looking at Large-Scale Moisture Transport and Its Relation to Amazonia and to Subtropical Rainfall in South America. *J Clim* **25**: 543–56.
- Barry RG. 2008. Mountain Weather and Climate Third Edition. Cambridge: Cambridge University Press.
- Beer C, Ciais P, Reichstein M, *et al.* 2009. Temporal and among-site variability of inherent water use efficiency at the ecosystem level. *Global Biogeochem Cycles* **23**.
- Bonan GB. 1998. The land surface climatology of the NCAR Land Surface Model coupled to the NCAR Community Climate Model. *J Clim* **11**: 1307–26.
- Bookhagen B and Strecker MR. 2008. Orographic barriers, high-resolution TRMM rainfall, and relief variations along the eastern Andes. *Geophys Res Lett* **35**: L06403.
- Bordon NG, Nogueira A, Leal Filho N, and Higuchi N. 2019. Blowdown disturbance effect on the density, richness and species composition of the seed bank in Central Amazonia. *For Ecol Manage* **453**: 117633.
- Borma LS, Rocha HR da, Cabral OM, *et al.* 2009. Atmosphere and hydrological controls of the evapotranspiration over a floodplain forest in the Bananal Island region, Amazonia. *J Geophys Res* **114**: G01003.
- Brando PM, Balch JK, Nepstad DC, *et al.* 2014. Abrupt increases in Amazonian tree mortality due to drought-fire interactions. *Proc Natl Acad Sci* **111**: 6347–52.
- Builes-Jaramillo A and Poveda G. 2018. Conjoint Analysis of Surface and Atmospheric Water Balances in the Andes-Amazon System. *Water Resour Res* **54**: 3472–89.
- Builes-Jaramillo A, Marwan N, Poveda G, and Kurths J. 2018a. Nonlinear interactions between the Amazon River basin and the Tropical North Atlantic at interannual timescales. *Clim Dyn* **50**: 2951–69.
- Builes-Jaramillo A, Ramos AMT, and Poveda G. 2018b. Atmosphere-Land Bridge between the Pacific and Tropical North Atlantic SST's through the Amazon River basin during the 2005 and 2010 droughts. *Chaos An Interdiscip J Nonlinear Sci* **28**: 085705.
- Buscardo E, Nardoto G, Luizão F, *et al.* 2016. The Biogeochemistry of the Main Forest Vegetation Types in Amazonia
- Cai W, McPhaden MJ, Grimm AM, *et al.* 2020. Climate impacts of the El Niño–Southern Oscillation on South America. *Nat Rev Earth Environ* **1**: 215–31.
- Campozano L, Céleri R, Trachte K, *et al.* 2016. Rainfall and Cloud Dynamics in the Andes: A Southern Ecuador Case Study. *Adv Meteorol* **2016**: 1–15.
- Campozano L, Trachte K, Céleri R, *et al.* 2018. Climatology and teleconnections of mesoscale convective systems in an Andean Basin in Southern Ecuador: The case of the Paute Basin. *Adv Meteorol* **2018**: 1–13.
- Carmona Duque AM. 2015. Impacts of climate change and climate variability on the spatio-temporal hydrological dynamics of Amazonia.
- Castello L and Macedo MN. 2015. Large-scale degradation of Amazonian freshwater ecosystems. *Glob Chang Biol* **22**: 990–1007.
- Chambers JQ, Negron-Juarez RI, Marra DM, *et al.* 2013. The steady-state mosaic of disturbance and succession

- across an old-growth Central Amazon forest landscape. *Proc Natl Acad Sci* **110**: 3949–54.
- Chambers JQ, Robertson AL, Carneiro VMC, *et al.* 2009. Hyperspectral remote detection of niche partitioning among canopy trees driven by blowdown gap disturbances in the Central Amazon. *Oecologia* **160**: 107–17.
- Chavez SP and Takahashi K. 2017. Orographic rainfall hot spots in the Andes-Amazon transition according to the TRMM precipitation radar and in situ data. *J Geophys Res Atmos* **122**: 5870–82.
- Christoffersen BO, Restrepo-Coupe N, Arain MA, *et al.* 2014. Mechanisms of water supply and vegetation demand govern the seasonality and magnitude of evapotranspiration in Amazonia and Cerrado. *Agric For Meteorol* **191**: 33–50.
- Coe MT, Costa MH, and Howard EA. 2008. Simulating the surface waters of the Amazon River basin: impacts of new river geomorphic and flow parameterizations. *Hydrol Process An Int J* **22**: 2542–53.
- Coelho C, Cavalcanti I, Ito R, *et al.* 2013. As secas de 1998, 2005 e 2010. Análise climatológica. *Secas na Amaz Causas e Consequências de Textos Press São Paulo*: 89–116.
- Cohen JCP, Silva Dias MAF and Nobre CA. 1995. Environmental conditions associated with Amazonian squall lines: A case study. *Mon Weather Rev* **123**: 3163–74.
- Costa MH, Biajoli MC, Sanches L, *et al.* 2010. Atmospheric versus vegetation controls of Amazonian tropical rain forest evapotranspiration: Are the wet and seasonally dry rain forests any different? *J Geophys Res* **115**: G04021.
- Costa MH and Foley JA. 1999. Trends in the hydrologic cycle of the Amazon Basin. *J Geophys Res Atmos* **104**: 14189–98.
- Costa MH, Souza-Filho JC, and Ribeiro A. 2004. Comments on “The Regional Evapotranspiration of the Amazon.” *J Hydrometeorol* **5**: 1279–80.
- Couto-Santos FR, Luizão FJ, and Carneiro Filho A. 2014. The influence of the conservation status and changes in the rainfall regime on forest-savanna mosaic dynamics in Northern Brazilian Amazonia. *Acta Amaz* **44**: 197–206.
- Cutrim EMC, Martin DW, Butzow DG, *et al.* 2000. Pilot Analysis of Hourly Rainfall in Central and Eastern Amazonia. *J Clim* **13**: 1326–34.
- da-Rocha HR, Manzi AO, Cabral OM, *et al.* 2009. Patterns of water and heat flux across a biome gradient from tropical forest to savanna in Brazil. *J Geophys Res* **114**: G00B12.
- da-Rocha HR, Goulden ML, Miller SD, *et al.* 2004. Seasonality of water and heat fluxes over a tropical forest in eastern Amazonia. *Ecol Appl* **14**: 22–32.
- de-Gonçalves LGG, Borak JS, Costa MH, *et al.* 2013. Overview of the large-scale biosphere-atmosphere experiment in Amazonia Data Model Intercomparison Project (LBA-DMIP). *Agric For Meteorol* **182**: 111–27.
- de-Oliveira AA De and Mori SA. 1999. A central Amazonian terra firme forest. I. High tree species richness on poor soils. *Biodivers Conserv* **8**: 1219–44.
- Debortoli NS, Dubreuil V, Funatsu B, *et al.* 2015. Rainfall patterns in the Southern Amazon: a chronological perspective (1971–2010). *Clim Change* **132**: 251–64.
- Deegan LA, Neill C, Hauptert CL, *et al.* 2011. Amazon deforestation alters small stream structure, nitrogen biogeochemistry and connectivity to larger rivers. *Biogeochemistry* **105**: 53–74.
- Dickinson RE, Oleson KW, Bonan G, *et al.* 2006. The Community Land Model and its climate statistics as a component of the Community Climate System Model. *J Clim* **19**: 2302–24.
- dos-Santos LT dos, Magnabosco Marra D, Trumbore S, *et al.* 2016. Windthrows increase soil carbon stocks in a central Amazon forest. *Biogeosciences* **13**: 1299–308.
- dos-Santos MJ dos, Silva Dias MAF, and Freitas ED. 2014. Influence of local circulations on wind, moisture, and precipitation close to Manaus City, Amazon Region, Brazil. *J Geophys Res Atmos* **119**: 13,233–13,249.
- Dowdy AJ and Mills GA. 2012. Atmospheric and fuel moisture characteristics associated with lightning-attributed fires. *J Appl Meteorol Climatol* **51**: 2025–37.
- Drumond A, Marengo J, Ambrizzi T, *et al.* 2014. The role of the Amazon Basin moisture in the atmospheric branch of the hydrological cycle: a Lagrangian analysis. *Hydrol Earth Syst Sci* **18**: 2577–98.
- Drumond A, Nieto R, Gimeno L, and Ambrizzi T. 2008. A Lagrangian identification of major sources of moisture over Central Brazil and La Plata Basin. *J Geophys Res Atmos* **113**.
- Egger J, Blacutt L, Ghezzi F, *et al.* 2005. Diurnal circulation of the Bolivian Altiplano. Part I: observations. *Mon Weather Rev* **133**: 911–24.
- Eltahir EAB and Pal JS. 1996. Relationship between surface conditions and subsequent rainfall in convective storms. *J Geophys Res Atmos* **101**: 26237–45.
- Espinoza JC, Chavez S, Ronchail J, *et al.* 2015. Rainfall hotspots over the southern tropical Andes: Spatial distribution, rainfall intensity, and relations with large-scale atmospheric circulation. *Water Resour Res* **51**: 3459–75.
- Espinoza JC, Garreaud R, Poveda G, *et al.* 2020. Hydroclimate of the Andes Part I: Main Climatic Features. *Front Earth Sci* **8**.
- Espinoza JC, Guyot JL, Ronchail J, *et al.* 2009a. Contrasting regional discharge evolutions in the Amazon basin (1974–2004). *J Hydrol* **375**: 297–311.
- Espinoza JC, Lengaigne M, Ronchail J, and Janicot S. 2012. Large-scale circulation patterns and related rainfall in the Amazon Basin: a neuronal networks approach. *Clim Dyn* **38**: 121–40.
- Espinoza JC, Marengo JA, Ronchail J, *et al.* 2014. The extreme 2014 flood in south-western Amazon basin: the role of tropical-subtropical South Atlantic SST gradient. *Environ Res Lett* **9**: 124007.
- Espinoza JC, Ronchail J, Guyot JL, *et al.* 2009b. Spatio-temporal rainfall variability in the Amazon basin countries (Brazil, Peru, Bolivia, Colombia, and Ecuador). *Int J Climatol* **29**: 1574–94.
- Espinoza JC, Ronchail J, Guyot JL, *et al.* 2011. Climate variability and extreme drought in the upper Solimões River (western Amazon Basin): Understanding the exceptional 2010 drought. *Geophys Res Lett* **38**: n/a-n/a.
- Espinoza JC, Ronchail J, Marengo JA, and Segura H. 2019. Contrasting North–South changes in Amazon wet-day and

- dry-day frequency and related atmospheric features (1981–2017). *Clim Dyn* **52**: 5413–30.
- Espinoza JC, Segura H, Ronchail J, *et al.* 2016. Evolution of wet-day and dry-day frequency in the western Amazon basin: Relationship with atmospheric circulation and impacts on vegetation. *Water Resour Res* **52**: 8546–60.
- Espinoza JC, Sörensson AA, Ronchail J, *et al.* 2019. Regional hydro-climatic changes in the Southern Amazon Basin (Upper Madeira Basin) during the 1982–2017 period. *J Hydrol Reg Stud* **26**: 100637.
- Espirito-Santo FDB, Keller M, Braswell B, *et al.* 2010. Storm intensity and old-growth forest disturbances in the Amazon region. *Geophys Res Lett* **37**: n/a–n/a.
- Figueroa M, Armijos E, Espinoza JC, *et al.* 2020. On the relationship between reversal of the river stage (repiquetes), rainfall and low-level wind regimes over the western Amazon basin. *J Hydrol Reg Stud* **32**: 100752.
- Figueroa SN and Nobre CA. 1990. Precipitation distribution over central and western tropical South America. *Climatol* **5**: 36–45.
- Figueroa SN, Satyamurty P, and Silva Dias PL Da. 1995. Simulations of the summer circulation over the South American region with an eta coordinate model. *J Atmos Sci* **52**: 1573–84.
- Fisher JB, Malhi Y, Bonal D, *et al.* 2009. The land–atmosphere water flux in the tropics. *Glob Chang Biol* **15**: 2694–714.
- Fitzjarrald DR, Sakai RK, Moraes OLL, *et al.* 2008. Spatial and temporal rainfall variability near the Amazon–Tapajós confluence. *J Geophys Res Biogeosciences* **113**.
- Foster DR, Knight DH, and Franklin JF. 1998. Landscape Patterns and Legacies Resulting from Large, Infrequent Forest Disturbances. *Ecosystems* **1**: 497–510.
- Fu R, Zhu B, and Dickinson RE. 1999. How do atmosphere and land surface influence seasonal changes of convection in the tropical Amazon? *J Clim* **12**: 1306–21.
- Fujita TT. 1990. Downbursts: meteorological features and wind field characteristics. *J Wind Eng Ind Aerodyn* **36**: 75–86.
- Fujita TT. 1981. Tornadoes and Downbursts in the Context of Generalized Planetary Scales. *J Atmos Sci* **38**: 1511–34.
- Garreaud RD, Vuille M, Compagnucci R, and Marengo J. 2009. Present-day South American climate. *Palaeogeogr Palaeoclimatol Palaeoecol* **281**: 180–95.
- Garstang M, White S, Shugart HH, and Halverson J. 1998. Convective cloud downdrafts as the cause of large blowdowns in the Amazon rainforest. *Meteorol Atmos Phys* **67**: 199–212.
- Garstang M and Fitzjarrald DR. 1999. Observations of surface to atmosphere interactions in the tropics. Oxford University Press, USA.
- Garstang M, Massie Jr HL, Halverson J, *et al.* 1994. Amazon coastal squall lines. Part I: Structure and kinematics. *Mon Weather Rev* **122**: 608–22.
- Gatti L V., Gloor M, Miller JB, *et al.* 2014. Drought sensitivity of Amazonian carbon balance revealed by atmospheric measurements. *Nature* **506**: 76–80.
- Germano MF and Oyama MD. 2020. Local Circulation Features in the Eastern Amazon: High-resolution Simulation. *J Aerosp Technol Manag* **12**.
- Germano MF, Vitorino MI, Cohen JCP, *et al.* 2017. Analysis of the breeze circulations in Eastern Amazon: an observational study. *Atmos Sci Lett* **18**: 67–75.
- Getirana AC V., Dutra E, Guimberteau M, *et al.* 2014. Water Balance in the Amazon Basin from a Land Surface Model Ensemble. *J Hydrometeorol* **15**: 2586–614.
- Gimeno L, Dominguez F, Nieto R, *et al.* 2016. Major mechanisms of atmospheric moisture transport and their role in extreme precipitation events. *Annu Rev Environ Resour* **41**: 117–41.
- Gimeno L, Vázquez M, Eiras-Barca J, *et al.* 2020. Recent progress on the sources of continental precipitation as revealed by moisture transport analysis. *Earth-Science Rev* **201**: 103070.
- Giovannettone JP and Barros AP. 2009. Probing Regional Orographic Controls of Precipitation and Cloudiness in the Central Andes Using Satellite Data. *J Hydrometeorol* **10**: 167–82.
- Gloor E, Wilson C, Chipperfield MP, *et al.* 2018. Tropical land carbon cycle responses to 2015/16 El Niño as recorded by atmospheric greenhouse gas and remote sensing data. *Philos Trans R Soc B Biol Sci* **373**: 20170302.
- Gloor M, Brienen RJW, Galbraith D, *et al.* 2013. Intensification of the Amazon hydrological cycle over the last two decades. *Geophys Res Lett* **40**: 1729–33.
- Gora EM, Burchfield JC, Muller-Landau HC, *et al.* 2020. Pantropical geography of lightning-caused disturbance and its implications for tropical forests. *Glob Chang Biol* **26**: 5017–26.
- Gotsch SG, Geiger EL, Franco AC, *et al.* 2010. Allocation to leaf area and sapwood area affects water relations of co-occurring savanna and forest trees. *Oecologia* **163**: 291–301.
- Goulding M, Barthelm R, and Ferreira EJG. 2003. The Smithsonian atlas of the Amazon.
- Greco S, Scala J, Halverson J, *et al.* 1994. Amazon coastal squall lines. Part II: Heat and moisture transports. *Mon Weather Rev* **122**: 623–35.
- Greco S, Swap R, Garstang M, *et al.* 1990. Rainfall and surface kinematic conditions over central Amazonia during ABLE 2B. *J Geophys Res Atmos* **95**: 17001–14.
- Gu G and Adler RF. 2019. Precipitation, temperature, and moisture transport variations associated with two distinct ENSO flavors during 1979–2014. *Clim Dyn* **52**: 7249–65.
- Hansen MC, Potapov P V, Moore R, *et al.* 2013. High-Resolution Global Maps of 21st-Century Forest Cover Change. *Science* **342**: 850–3.
- Hasler N and Avissar R. 2007. What Controls Evapotranspiration in the Amazon Basin? *J Hydrometeorol* **8**: 380–95.
- Hess LL, Melack JM, Affonso AG, *et al.* 2015. Wetlands of the lowland Amazon basin: Extent, vegetative cover, and dual-season inundated area as mapped with JERS-1 synthetic aperture radar. *Wetlands* **35**: 745–56.
- Hirota M, Nobre C, Oyama MD, and Bustamante MM. 2010. The climatic sensitivity of the forest, savanna and forest-savanna transition in tropical South America. *New Phytol* **187**: 707–19.
- Hodnett MG, Vendrame I, O. Marques Filho A De, *et al.* 1997. Soil water storage and groundwater behaviour in a catena

- sequence beneath forest in central Amazonia: I. Comparisons between plateau, slope and valley floor. *Hydrol Earth Syst Sci* **1**: 265–77.
- Hoffmann WA, Adasme R, Haridasan M, *et al.* 2009. Tree topkill, not mortality, governs the dynamics of savanna–forest boundaries under frequent fire in central Brazil. *Ecology* **90**: 1326–37.
- Hoffmann WA, Geiger EL, Gotsch SG, *et al.* 2012. Ecological thresholds at the savanna-forest boundary: how plant traits, resources and fire govern the distribution of tropical biomes (F Lloret, Ed). *Ecol Lett* **15**: 759–68.
- Horel JD, Hahmann AN, and Geisler JE. 1989. An investigation of the annual cycle of convective activity over the tropical Americas. *J Clim* **2**: 1388–403.
- House JJ, Archer S, Breshears DD, and Scholes RJ. 2003. Conundrums in mixed woody-herbaceous plant systems. *J Biogeogr* **30**: 1763–77.
- Houze Jr RA. 2012. Orographic effects on precipitating clouds. *Rev Geophys* **50**.
- Hoyos I, Dominguez F, Cañón-Barriga J, *et al.* 2017. Moisture origin and transport processes in Colombia, northern South America. *Clim Dyn* **50**: 971–90.
- Huggel C, Raissig A, Rohrer M, *et al.* 2015. How useful and reliable are disaster databases in the context of climate and global change? A comparative case study analysis in Peru. *Nat Hazards Earth Syst Sci* **15**: 475–85.
- Hutyra LR, Munger JW, Nobre CA, *et al.* 2005. Climatic variability and vegetation vulnerability in Amazônia. *Geophys Res Lett* **32**: L24712.
- IPCC Climate Change. 2014. Synthesis Report - Contribution of Working groups I, II and III to the Fifth Assessment Report of the Intergovernmental Panel on Climate Change.
- Jiménez-Muñoz JC, Marengo JA, Alves LM, *et al.* (2021). The role of ENSO flavours and TNA on recent droughts over Amazon forests and the Northeast Brazil region. *Int J Climatol* **41**: 3761–80.
- Jiménez-Muñoz JC, Barichivich J, Mattar C, *et al.* 2018. Spatio-temporal patterns of thermal anomalies and drought over tropical forests driven by recent extreme climatic anomalies. *Philos Trans R Soc B Biol Sci* **373**: 20170300.
- Jiménez-Muñoz JC, Mattar C, Barichivich J, *et al.* 2016. Record-breaking warming and extreme drought in the Amazon rainforest during the course of El Niño 2015–2016. *Sci Rep* **6**: 1–7.
- Jiménez-Sánchez G, Markowski PM, Jewtoukoff V, *et al.* 2019. The Orinoco Low-Level Jet: An Investigation of Its Characteristics and Evolution Using the WRF Model. *J Geophys Res Atmos* **124**: 10696–711.
- Jones C. 2019. Recent changes in the South America low-level jet. *npj Clim Atmos Sci* **2**: 20.
- Jones C and Carvalho LM V. 2018. The influence of the Atlantic multidecadal oscillation on the eastern Andes low-level jet and precipitation in South America. *NPJ Clim Atmos Sci* **1**: 1–7.
- Juárez RIN, Hodnett MG, Fu R, *et al.* 2007. Control of Dry Season Evapotranspiration over the Amazonian Forest as Inferred from Observations at a Southern Amazon Forest Site. *J Clim* **20**: 2827–39.
- Junk WJ, Piedade MTF, Schöngart J, and Wittmann F. 2012. A classification of major natural habitats of Amazonian white-water river floodplains (várzeas). *Wetl Ecol Manag* **20**: 461–75.
- Junquas C, Li L, Vera CS, *et al.* 2015. Influence of South America orography on summertime precipitation in Southeastern South America. *Clim Dyn* **46**: 3941–63.
- Junquas C, Takahashi K, Condom T, *et al.* 2018. Understanding the influence of orography on the precipitation diurnal cycle and the associated atmospheric processes in the central Andes. *Clim Dyn* **50**: 3995–4017.
- Kayano MT and Capistrano VB. 2014. How the Atlantic multidecadal oscillation (AMO) modifies the ENSO influence on the South American rainfall. *Int J Climatol* **34**: 162–78.
- Keller M, Alencar A, Asner GP, *et al.* 2004. Ecological research in the large-scale biosphere-atmosphere experiment in Amazonia: early results. *Ecol Appl* **14**: 3–16.
- Kousky VE. 1980. Diurnal rainfall variation in northeast Brazil. *Mon Weather Rev* **108**: 488–98.
- Kumar S, Moya-Álvarez AS, Castillo-Velarde C Del, *et al.* 2020. Effect of low-level flow and Andes mountain on the tropical and mid-latitude precipitating cloud systems: GPM observations. *Theor Appl Climatol* **141**: 157–72.
- Laraque A, Ronchail J, Cochonneau G, *et al.* 2007. Heterogeneous Distribution of Rainfall and Discharge Regimes in the Ecuadorian Amazon Basin. *J Hydrometeorol* **8**: 1364–81.
- Lavado-Casimiro WS, Ronchail J, Labat D, *et al.* 2012. Basin-scale analysis of rainfall and runoff in Peru (1969–2004): Pacific, Titicaca and Amazonas drainages. *Hydrol Sci J* **57**: 625–42.
- Lavado-Casimiro W and Espinoza JC. 2014. Impactos de El Niño y La Niña en las lluvias del Perú (1965–2007). *Rev Bras Meteorol* **29**: 171–82.
- Lenters JD and Cook KH. 1997. On the Origin of the Bolivian High and Related Circulation Features of the South American Climate. *J Atmos Sci* **54**: 656–78.
- Leopoldo PR, Franken W, Salati E, and Ribeiro MN. 1987. Towards a water balance in the Central Amazonian region. *Experientia* **43**: 222–33.
- Lesack LW and Melack J. 1996. Mass balance of major solutes in a rainforest catchment in the Central Amazon: Implications for nutrient budgets in tropical rainforests. *Biogeochemistry* **32**.
- Lewis SL, Brando PM, Phillips OL, *et al.* 2011. The 2010 amazon drought. *Science* **331**: 554.
- Liebmann B and Mechoso CR. 2011. The South American Monsoon System. In: Chih-Pei Chang *et al.* (Ed). The Global Monsoon System: Research and Forecast, 2nd Edition. World Scientific Series on Asia-Pacific Weather and Climate. The Global Monsoon System.
- Liebmann B, Camargo SJ, Seth A, *et al.* 2007. Onset and end of the rainy season in South America in observations and the ECHAM 4.5 atmospheric general circulation model. *J Clim* **20**: 2037–50.
- Liebmann B and Marengo J. 2001. Interannual Variability of the Rainy Season and Rainfall in the Brazilian Amazon Basin. *J Clim* **14**: 4308–18.

- Liebmann B and Smith CA. 1996. Description of a complete (interpolated) outgoing longwave radiation dataset. *Bull Am Meteorol Soc* **77**: 1275–7.
- Lloyd J, Goulden ML, Ometto JP, *et al.* 2009. Ecophysiology of forest and savanna vegetation. In: Geophysical Monograph Series.
- Magnabosco Marra D, Chambers JQ, Higuchi N, *et al.* 2014. Large-Scale Wind Disturbances Promote Tree Diversity in a Central Amazon Forest (HYH Chen, Ed). *PLoS One* **9**: e103711.
- Magnabosco Marra D, Trumbore SE, Higuchi N, *et al.* 2018. Windthrows control biomass patterns and functional composition of Amazon forests. *Glob Chang Biol* **24**: 5867–81.
- Marengo JA, Liebmann B, Grimm AM, *et al.* 2012. Recent developments on the South American monsoon system. *Int J Climatol* **32**: 1–21.
- Marengo JA. 2005. Characteristics and spatio-temporal variability of the Amazon River Basin Water Budget. *Clim Dyn* **24**: 11–22.
- Marengo JA, Nobre CA, Tomasella J, *et al.* 2008. The Drought of Amazonia in 2005. *J Clim* **21**: 495–516.
- Marengo JA, Tomasella J, Alves LM, *et al.* 2011. The drought of 2010 in the context of historical droughts in the Amazon region. *Geophys Res Lett* **38**.
- Marengo JA, Alves LM, Soares WR, *et al.* 2013. Two contrasting severe seasonal extremes in tropical South America in 2012: flood in Amazonia and drought in northeast Brazil. *J Clim* **26**: 9137–54.
- Marengo JA, Soares WR, Saulo C, and Nicolini M. 2004. Climatology of the low-level jet east of the Andes as derived from the NCEP–NCAR reanalyses: Characteristics and temporal variability. *J Clim* **17**: 2261–80.
- Marengo JA, Souza Jr CM, Thonicke K, *et al.* 2018. Changes in climate and land use over the Amazon region: current and future variability and trends. *Front Earth Sci* **6**: 228.
- Marengo JA and Espinoza JC. 2016. Extreme seasonal droughts and floods in Amazonia: causes, trends and impacts. *Int J Climatol* **36**: 1033–50.
- Marra DM, Fagg CW, Pereira BA da S, and Felfili JM. 2014. Árvores e variáveis ambientais influenciam a regeneração natural de uma floresta estacional decidual no Brasil Central. *Neotrop Biol Conserv* **9**.
- Martinelli LA, Coletta LD, Ravagnani EC, *et al.* 2010. Dissolved nitrogen in rivers: comparing pristine and impacted regions of Brazil. *Brazilian J Biol* **70**: 709–22.
- Matos AP and Cohen JCP. 2016. Circulação de Brisa Fluvial e a Banda de Precipitação na Margem Leste da Baía De Marajó. *Ciência e Nat* **38**: 21.
- Mayta VC, Ambrizzi T, Espinoza JC, and Silva Dias PL. 2018. The role of the Madden-Julian oscillation on the Amazon Basin intraseasonal rainfall variability. *Int J Climatol* **39**: 343–60.
- McClain ME and Naiman RJ. 2008. Andean influences on the biogeochemistry and ecology of the Amazon River. *Bioscience* **58**: 325–38.
- McDowell N, Allen CD, Anderson-Teixeira K, *et al.* 2018. Drivers and mechanisms of tree mortality in moist tropical forests. *New Phytol* **219**: 851–69.
- Medeiros PM, Seidel M, Ward ND, *et al.* 2015. Fate of the Amazon River dissolved organic matter in the tropical Atlantic Ocean. *Global Biogeochem Cycles* **29**: 677–90.
- Melack JM and Coe MT. 2013. Climate change and the Floodplain Lakes of the Amazon Basin. *Amaz Glob Chang (eds Goldman CR, Kumagai M, Robarts R)*: 295–310.
- Miller STK. 2003. Sea breeze: Structure, forecasting, and impacts. *Rev Geophys* **41**: 1011.
- Mitchell SJ. 2013. Wind as a natural disturbance agent in forests: a synthesis. *Forestry* **86**: 147–57.
- Molina-Carpio J, Espinoza JC, Vauchel P, *et al.* 2017. Hydroclimatology of the Upper Madeira River basin: spatio-temporal variability and trends. *Hydrol Sci J* **62**: 911–27.
- Moquet J-S, Crave A, Viers J, *et al.* 2011. Chemical weathering and atmospheric/soil CO₂ uptake in the Andean and Foreland Amazon basins. *Chem Geol* **287**: 1–26.
- Nauslar N, Kaplan M, Wallmann J, and Brown T. 2013. A forecast procedure for dry thunderstorms. *J Oper Meteorol* **1**: 200–14.
- Navarro-Monterroza E, Arias PA, and Vieira SC. 2019. El Niño-Oscilación del Sur, fase Modoki, y sus efectos en la variabilidad espacio-temporal de la precipitación en Colombia. *Rev la Acad Colomb Ciencias Exactas, Físicas y Nat* **43**: 120.
- Negrón-Juárez RI, Chambers JQ, Guimaraes G, *et al.* 2010. Widespread Amazon forest tree mortality from a single cross-basin squall line event. *Geophys Res Lett* **37**: n/a-n/a.
- Negrón-Juárez RI, Chambers JQ, Marra DM, *et al.* 2011. Detection of subpixel treefall gaps with Landsat imagery in Central Amazon forests. *Remote Sens Environ* **115**: 3322–8.
- Negrón-Juárez RI, Holm JA, Marra DM, *et al.* 2018. Vulnerability of Amazon forests to storm-driven tree mortality. *Environ Res Lett* **13**: 54021.
- Negrón-Juárez R, Jenkins H, Raupp C, *et al.* 2017. Windthrow Variability in Central Amazonia. *Atmosphere (Basel)* **8**: 28.
- Nelson BW. 1994. Natural forest disturbance and change in the Brazilian Amazon. *Remote Sens Rev* **10**: 105–25.
- Nelson BW, Kapos V, Adams JB, *et al.* 1994. Forest disturbance by large blowdowns in the Brazilian Amazon. *Ecology* **75**: 853–8.
- Nobre CA, Sampaio G, Borma LS, *et al.* 2016. Land-use and climate change risks in the Amazon and the need of a novel sustainable development paradigm. *Proc Natl Acad Sci* **113**: 10759–68.
- Nobre CA, Sellers PJ, and Shukla J. 1991. Amazonian Deforestation and Regional Climate Change. *J Clim* **4**: 957–88.
- Ovando A, Tomasella J, Rodriguez DA, *et al.* 2016. Extreme flood events in the Bolivian Amazon wetlands. *J Hydrol Reg Stud* **5**: 293–308.
- Paiva RCD, Buarque DC, Clarke RT, *et al.* 2011. Reduced precipitation over large water bodies in the Brazilian Amazon shown from TRMM data. *Geophys Res Lett* **38**.
- Peterson CJ, Ribeiro GHP de M, Negrón-Juárez R, *et al.* 2019. Critical wind speeds suggest wind could be an important disturbance agent in Amazonian forests. *For An Int J For Res* **92**: 444–59.

- Piedade MTF, Worbes M, and Junk WJ. 2001. Geoecological Controls on Elemental Fluxes in Communities of Higher Plants. *Biogeochem Amaz Basin*: 209.
- Planchon O, Damato F, Dubreuil V, and Gouéry P. 2006. A method of identifying and locating sea-breeze fronts in north-eastern Brazil by remote sensing. *Meteorol Appl A J Forecast Pract Appl Train Tech Model* **13**: 225–34.
- Poveda G, Espinoza JC, Zuluaga MD, et al. 2020. High Impact Weather Events in the Andes. *Front Earth Sci* **8**.
- Poveda G, Jaramillo L, and Vallejo LF. 2014. Seasonal precipitation patterns along pathways of South American low-level jets and aerial rivers. *Water Resour Res* **50**: 98–118.
- Poveda G, Mesa OJ, Salazar LF, et al. 2005. The diurnal cycle of precipitation in the tropical Andes of Colombia. *Mon Weather Rev* **133**: 228–40.
- Poveda G, Waylen PR, and Pulwarty RS. 2006. Modern climate variability in northern South America and southern Mesomerica. *Palaeogeogr Palaeoclimatol Palaeoecol* **234**: 3–27.
- Ramos-Neto MB and Pivello VR. 2000. Lightning fires in a Brazilian savanna National Park: rethinking management strategies. *Environ Manage* **26**: 675–84.
- Rao VB and Hada K. 1990. Characteristics of rainfall over Brazil: Annual variations and connections with the Southern Oscillation. *Theor Appl Climatol* **42**: 81–91.
- Rao VB, Franchito SH, Santo CME, and Gan MA. 2016. An update on the rainfall characteristics of Brazil: seasonal variations and trends in 1979–2011. *Int J Climatol* **36**: 291–302.
- Ratnam J, Bond WJ, Fensham RJ, et al. 2011. When is a ‘forest’ a savanna, and why does it matter? *Glob Ecol Biogeogr* **20**: 653–60.
- Ribeiro GHM, Chambers JQ, Peterson CJ, et al. 2016. Mechanical vulnerability and resistance to snapping and uprooting for Central Amazon tree species. *For Ecol Manage* **380**: 1–10.
- Ribeiro M de NG and Adis J. 1984. Local rainfall variability—A potential bias for bioecological studies in the Central Amazon. *Acta Amaz* **14**: 159–74.
- Ricarte RMD, Herdies DL, and Barbosa TF. 2014. Patterns of atmospheric circulation associated with cold outbreaks in southern Amazonia. *Meteorol Appl* **22**: 129–40.
- Richey JE, Nobre C, and Deser C. 1989. Amazon River Discharge and Climate Variability: 1903 to 1985. *Science* **246**: 101–3.
- Rifai SW, Urquiza Muñoz JD, Negrón-Juárez RI, et al. 2016. Landscape-scale consequences of differential tree mortality from catastrophic wind disturbance in the Amazon. *Ecol Appl* **26**: 2225–37.
- Roe GH. 2005. Orographic precipitation. *Annu Rev Earth Planet Sci* **33**: 645–71.
- Rollenbeck R and Bendix J. 2011. Rainfall distribution in the Andes of southern Ecuador derived from blending weather radar data and meteorological field observations. *Atmos Res* **99**: 277–89.
- Romatschke U and Houze RA. 2013. Characteristics of precipitating convective systems accounting for the summer rainfall of tropical and subtropical South America. *J Hydrometeorol* **14**: 25–46.
- Ronchail J, Cochonneau G, Molinier M, et al. 2002. Interannual rainfall variability in the Amazon basin and sea-surface temperatures in the equatorial Pacific and the tropical Atlantic Oceans. *Int J Climatol* **22**: 1663–86.
- Saavedra M, Junquas C, Espinoza J-C, and Silva Y. 2020. Impacts of topography and land use changes on the air surface temperature and precipitation over the central Peruvian Andes. *Atmos Res* **234**: 104711.
- Salati E, Dall’Olio A, Matsui E, and Gat JR. 1979. Recycling of water in the Amazon Basin: An isotopic study. *Water Resour Res* **15**: 1250–8.
- Salazar Villegas JF, Poveda GJ, and Salazar LFV. 2004. Balances hidrológicos y estimación de caudales extremos en la Amazonia.
- Schwartz NB, Uriarte M, DeFries R, et al. 2017. Fragmentation increases wind disturbance impacts on forest structure and carbon stocks in a western Amazonian landscape. *Ecol Appl* **27**: 1901–15.
- Segura H, Espinoza JC, Junquas C, et al. 2020. Recent changes in the precipitation-driving processes over the southern tropical Andes/western Amazon. *Clim Dyn*: 1–19.
- Segura H, Junquas C, Espinoza JC, et al. 2019. New insights into the rainfall variability in the tropical Andes on seasonal and interannual time scales. *Clim Dyn* **53**: 405–26.
- Shuttleworth WJ. 1988. Evaporation from Amazonian rainforest. *Proc R Soc London Ser B Biol Sci* **233**: 321–46.
- Silva Dias MAF, Silva Dias PL, Longo M, et al. 2004. River breeze circulation in eastern Amazonia: observations and modelling results. *Theor Appl Climatol* **78**.
- Silva Dias MA. 1987. Sistemas de Mesoescala e Previsão de Tempo à Curto Prazo. *Rev Bras Meteorol* **2**: 133–57.
- Silva Dias PL, Schubert WH, and De Maria M. 1983. Large-scale response of the tropical atmosphere to transient convection. *J Atmos Sci* **40**: 2689–707.
- Silva Y, Takahashi K, and Chávez R. 2008. Dry and wet rainy seasons in the Mantaro river basin (Central Peruvian Andes). *Adv Geosci* **14**: 261–4.
- Silvério D V., Brando PM, Bustamante MMC, et al. 2019. Fire, fragmentation, and windstorms: A recipe for tropical forest degradation (D Edwards, Ed). *J Ecol* **107**: 656–67.
- Smith NJH. 2002. Amazon sweet sea: land, life, and water at the river’s mouth. University of Texas Press.
- Sommer R, Fölster H, Vielhauer K, et al. 2003. Deep soil water dynamics and depletion by secondary vegetation in the Eastern Amazon. *Soil Sci Soc Am J* **67**: 1672–86.
- Sorribas MV, Paiva RCD, Melack JM, et al. 2016. Projections of climate change effects on discharge and inundation in the Amazon basin. *Clim Change* **136**: 555–70.
- Souza Filho PWM. 2005. Costa de manguezais de macromaré da Amazônia: Cenários morfológicos, mapeamento e quantificação de áreas usando dados de sensores remotos. *Rev Bras Geofísica* **23**: 427–35.
- Souza EB and Ambrizzi T. 2006. Modulation of the intraseasonal rainfall over tropical Brazil by the Madden–Julian oscillation. *Int J Climatol* **26**: 1759–76.
- Staal A, Tuinenburg OA, Bosmans JHC, et al. 2018. Forest-rainfall cascades buffer against drought across the Amazon. *Nat Clim Chang* **8**: 539–43.

- Sulca J, Takahashi K, Espinoza J-C, *et al.* 2018. Impacts of different ENSO flavors and tropical Pacific convection variability (ITCZ, SPCZ) on austral summer rainfall in South America, with a focus on Peru. *Int J Climatol* **38**: 420–35.
- Takahashi K, Montecinos A, Goubanova K, and Dewitte B. 2011. ENSO regimes: Reinterpreting the canonical and Modoki El Niño. *Geophys Res Lett* **38**.
- Tedeschi RG and Collins M. 2017. The influence of ENSO on South American precipitation: simulation and projection in CMIP5 models. *Int J Climatol* **37**: 3319–39.
- Torello-Raventos M, Feldpausch TR, Veenendaal E, *et al.* 2013. On the delineation of tropical vegetation types with an emphasis on forest/savanna transitions. *Plant Ecol & Divers* **6**: 101–37.
- Trachte K, Rollenbeck R, and Bendix J. 2010a. Nocturnal convective cloud formation under clear-sky conditions at the eastern Andes of south Ecuador. *J Geophys Res Atmos* **115**.
- Trachte K, Nauss T, and Bendix J. 2010b. The impact of different terrain configurations on the formation and dynamics of katabatic flows: Idealised case studies. *Boundary-layer Meteorol* **134**: 307–25.
- Trumbore S, Brando P, and Hartmann H. 2015. Forest health and global change. *Science* **349**: 814–8.
- Turner MG. 2010. Disturbance and landscape dynamics in a changing world. *Ecology* **91**: 2833–49.
- Vauchel P, Santini W, Guyot JL, *et al.* 2017. A reassessment of the suspended sediment load in the Madeira River basin from the Andes of Peru and Bolivia to the Amazon River in Brazil, based on 10 years of data from the HYBAM monitoring programme. *J Hydrol* **553**: 35–48.
- Vera C, Baez J, Douglas M, *et al.* 2006b. The South American low-level jet experiment. *Bull Am Meteorol Soc* **87**: 63–78.
- Vera C, Higgins W, Amador J, *et al.* 2006a. Toward a Unified View of the American Monsoon Systems. *J Clim* **19**: 4977–5000.
- Viana LP and Herdies DL. 2018. Case Study of a Cold air Outbreak Incursion Extreme Event in July 2013 on Brazilian Amazon Basin. *Rev Bras Meteorol* **33**: 27–39.
- Viegas DX. 2012. Extreme fire behaviour. *For Manag Technol Pract Impact*: 1–56.
- Vourlitis GL, Filho NP, Hayashi MMS, *et al.* 2002. Seasonal variations in the evapotranspiration of a transitional tropical forest of Mato Grosso, Brazil. *Water Resour Res* **38**: 30–1.
- Wallace JM and Hobbs P V. 2006. Atmospheric science: an introductory survey. Elsevier.
- Wanzeler RTS. 2018. Períodos ativos e inativos da brisa nas regiões do Centro de Lançamento de Alcântara e de Belém/PA durante o período seco.
- Weng W, Luedeke MKB, Zemp DC, *et al.* 2018. Aerial and surface rivers: downwind impacts on water availability from land use changes in Amazonia. *Hydrol Earth Syst Sci* **22**: 911–27.
- Werth D and Avissar R. 2004. The regional evapotranspiration of the Amazon. *J Hydrometeorol* **5**: 100–9.
- Wilcke W, Leimer S, Peters T, *et al.* 2013. The nitrogen cycle of tropical montane forest in Ecuador turns inorganic under environmental change. *Global Biogeochem Cycles* **27**: 1194–204.
- Wilcke W, Oelmann Y, Schmitt A, *et al.* 2008. Soil properties and tree growth along an altitudinal transect in Ecuadorian tropical montane forest. *J Plant Nutr Soil Sci* **171**: 220–30.
- Williams E, Dall' Antonia A, Dall' Antonia V, *et al.* 2005. The drought of the century in the Amazon Basin: an analysis of the regional variation of rainfall in South America in 1926. *Acta Amaz* **35**: 231–8.
- Williams MR and Melack JM. 1997. Solute export from forested and partially deforested catchments in the central Amazon. *Biogeochemistry* **38**: 67–102.
- Yanoviak SP, Gora EM, Bitzer PM, *et al.* 2020. Lightning is a major cause of large tree mortality in a lowland neotropical forest. *New Phytol* **225**: 1936–44.
- Zeng N. 1999. Seasonal cycle and interannual variability in the Amazon hydrologic cycle. *J Geophys Res Atmos* **104**: 9097–106.
- Zeng N, Yoon J-H, Marengo JA, *et al.* 2008. Causes and impacts of the 2005 Amazon drought. *Environ Res Lett* **3**: 14002.
- Zheleznova IV and Gushchina DY. 2017. Hadley and Walker circulation anomalies associated with the two types of El Niño. *Russ Meteorol Hydrol* **42**: 625–34.
- Zhou J and Lau KM. 1998. Does a monsoon climate exist over South America? *J Clim* **11**: 1020–40.

CONTACT INFORMATION

SPA Technical-Scientific Secretariat New York

475 Riverside Drive, Suite 530

New York NY 10115

USA

+1 (212) 870-3920

spa@unsdsn.org

SPA Technical-Scientific Secretariat South America

Av. Ironman Victor Garrido, 623

São José dos Campos – São Paulo

Brazil

spasouthamerica@unsdsn.org

WEBSITE theamazonwewant.org

INSTAGRAM [@theamazonwewant](https://www.instagram.com/theamazonwewant)

TWITTER [@theamazonwewant](https://twitter.com/theamazonwewant)